



HAL
open science

Soft Landing Mass-Selected Ions for Single Molecule Imaging

Xiaocui Wu, Dhaneesh Kumar, Jimin Ham, Shengpeng Huang, Kelvin Anggara

► **To cite this version:**

Xiaocui Wu, Dhaneesh Kumar, Jimin Ham, Shengpeng Huang, Kelvin Anggara. Soft Landing Mass-Selected Ions for Single Molecule Imaging. American Chemical Society, 2025, ACS In Focus, 9780841296121. <10.1021/acsinfocus.7e9004>. <hal-05453448>

HAL Id: hal-05453448

<https://hal.science/hal-05453448v1>

Submitted on 20 Jan 2026

HAL is a multi-disciplinary open access archive for the deposit and dissemination of scientific research documents, whether they are published or not. The documents may come from teaching and research institutions in France or abroad, or from public or private research centers.

L'archive ouverte pluridisciplinaire HAL, est destinée au dépôt et à la diffusion de documents scientifiques de niveau recherche, publiés ou non, émanant des établissements d'enseignement et de recherche français ou étrangers, des laboratoires publics ou privés.



HAL Authorization

Soft Landing Mass-Selected Ions for Single Molecule Imaging

Xiaocui Wu, Dhaneesh Kumar, Jimin Ham, Shengpeng Huang, Kelvin Anggara

Table of Contents

1	1. Introduction	3
2	1.1. ESIBD enables single molecule analysis of biomolecules.....	11
3	1.2. ESIBD enables preparation of self-assembled nanostructures on surface	15
4	1.3. ESIBD roadmap.....	20
5	1.3.1. Ion transmission at atmosphere-vacuum interface	20
6	1.3.2. Selection of ion shape	21
7	1.4. Next chapters	21
8	1.5. Read these next	22
9	2. The electrospray ionization	24
10	2.1. Introduction: Giving wings to molecular elephants	24
11	2.2. How it works: From liquid jets to single ions.....	27
12	2.3. ESI in practice	31
13	2.3.1. The emitter.....	32
14	2.3.2. The sample solution	34
15	2.4. Read these next	38
16	3. The mass selection in vacuum	39
17	3.1. Introduction: Designing a filter for ions.....	39
18	3.2. Vacuum basics.....	41
19	3.2.1. Establishing vacuum.....	43
20	3.2.2. Differential pumping.....	44
21	3.3. Ion manipulation in vacuum.....	46
22	3.3.1. Kinetic energies of ions	46
23	3.3.2. Electrostatic lenses (Einzel lenses)	47
24	3.3.3. Electrostatic steering plates	49
25	3.4. Quadrupole mass selection.....	50
26	3.4.1. <i>m/z</i> mass selection: how does it work?.....	51
27	3.4.2. Quadrupole arrangement and principles.....	52
28	3.4.3. First stability region	55

33	3.4.4. Trade-offs	57
34	4. The soft landing	59
35	4.1. Introduction: Parachuting ions onto surfaces	59
36	4.2. How it works: Setting the touchdown speed and direction	60
37	4.2.1. Collision energy	61
38	4.2.2. Collision angle	63
39	4.3. What happens to ions during and after landing?	64
40	4.4. Soft landing in practice	67
41	4.4.1. The landing energy	67
42	4.4.2. The deposition time	70
43	4.4.3. The surface choice	70
44	4.5. The future of the field	74
45	4.6. Read these next	75
46		
47		

48 **Preface**

49

50 Dear Reader,

51

52 As authors, we want you to learn something from this primer.

53

54 We thus owe it to you to be clear from the start on what this primer is about and how it can help
55 you.

56

57 This primer focuses on bridging two seemingly distant technologies – mass spectrometry and
58 single molecule imaging – with a technique called “soft landing.” This combination offers unique
59 solutions and opportunities that could not be realized by either of them alone: it allows molecules
60 you have worked so hard to prepare to be directly imaged one-molecule-at-a-time.

61

62 You may have heard of mass spectrometry as a technique that identifies molecules by measuring
63 their molecular mass. You also may have heard of single molecule imaging techniques, such as
64 scanning probe microscopy and transmission electron microscopy, which are two direct imaging
65 techniques today capable of imaging, with atomic resolution, the structures of individual molecules
66 adsorbed on surfaces in vacuum.

67

68 Now you will learn how to combine mass spectrometry and single molecule imaging into a single
69 workflow.

70

71 “But, why?” you ask. Because, by doing so, we can now transfer molecules initially in solutions
72 onto surfaces in vacuum so that they can be imaged one-at-a-time. Direct imaging of single
73 molecules allows you to determine the diverse structures and interactions of complex molecules
74 at the ultimate single molecule level. This is a feat that is beyond the reach of today’s analytical
75 techniques – which analyze millions of molecules at a time (also known as ensemble averaging)
76 and hence obscure the rich chemical information at the individual level.

77

78 To accomplish this, we discuss three key steps in this workflow: how to bring complex molecules
79 from solutions into the gas phase as ions using electrospray ionization (Chapter 2), how to select
80 them in the gas phase based on their mass-to-charge ratios (Chapter 3), and how to land them
81 intact on surfaces for their direct single molecule imaging (Chapter 4). We write the primer to
82 emphasize the main ideas and the mental models we use to understand, refine, and troubleshoot
83 these three key steps.

84

85 Our hope is that this primer bridges the first time learners and the survey literature in the field,
86 e.g., textbooks and reviews, which we provide as a reading list at the end of every chapter.
87 Focusing on clarity over completeness, we write the primer not as an in-depth review of the field,
88 but as a “travel guide” for prospective tourists to the field. For those familiar with mass
89 spectrometry, you will learn a way to soft land and direct image the molecular ions you are
90 studying in the gas phase. For those familiar with microscopy on surfaces, you will learn a way to
91 prepare contaminant-free samples of complex molecules isolated from solution phase. For

92 newcomers to both fields, you will learn an analytical tool that allows molecules in solutions to be
93 isolated in gas phase, landed onto surfaces in vacuum, and imaged one-at-a-time for their single
94 molecule structural analysis.

95
96 This primer focuses on single molecule analysis of soft landed molecules isolated from solutions
97 by electrospray ionization. We note however that this is not the sole application of soft landing
98 technique, which by itself finds wide applications beyond those covered in this primer, such as
99 surface deposition of metal or metal oxide cluster ions on self-assembled monolayers or electrode
100 surfaces for thin film material fabrication. We further note that ions can be generated by
101 techniques, alternative to electrospray ionization, such as laser ablation, matrix desorption,
102 magnetron sputtering, etc.

103
104 We will be thrilled to hear your feedback, be that clarification on specific points or even your ideas
105 on how to make things better. We ask that you to not hesitate to reach out to one of us.

106
107 To close, in the Biographical Memoirs for John B. Fenn describing his work on electrospray
108 ionization of macromolecules to which he was awarded the 2002 Nobel Prize in Chemistry,
109 Charles E. Kolb wrote:

110
111 *Like Disney's Dumbo did before.*
112 *Elephant ions learned to fly.*

113
114 It is time they learn how to land.

115
116 Best wishes,

117
118 The Authors

119
120

121 **Author biographies**

122 Xiaocui Wu is a postdoctoral researcher in the Nanoscale Science Department at the Max Planck
123 Institute for Solid State Research. She is currently working on single molecule imaging of
124 polysaccharides soft landed on metal surfaces by electrospray ion beam deposition. She received
125 her B.Sc. and M.Sc. degrees in nuclear engineering from Sun Yat-sen University, China, and
126 Ph.D. in physical chemistry from Université Paris Sciences et Lettres, France, in 2020. She
127 continued her research as postdoctoral fellow at Technische Universität Ilmenau in Germany and
128 then at University of Warwick as Marie Curie Cofund fellow in the United Kingdom before joining
129 Max Planck Institute for Solid State Research.

130
131 Dhaneesh Kumar is a postdoctoral researcher in the Nanoscale Science Department at the Max
132 Planck Institute for Solid State Research. He is currently working on single molecule imaging and
133 spectroscopy, via scanning tunneling microscopy, of biomolecules soft landed on metal surfaces
134 by means of electrospray ion beam deposition. He received his B.Sc. degree in Physics and
135 Mathematics from the University of British Columbia, Vancouver, Canada. He obtained his Ph.D

136 in Physics from Monash University, Australia in 2021 where he focused on studying the structural
137 and electronic properties of low-dimensional organic nanostructures on surfaces using scanning
138 tunneling microscopy before joining Max Planck Institute for Solid State Research.

139
140 Jimin Ham is a postdoctoral researcher in the Nanoscale Science Department at the Max Planck
141 Institute for Solid State Research. She is interested in imaging and material synthesis at the
142 nanoscale. She is currently studying structures of single protonated molecules deposited by
143 electrospray ion beam deposition with scanning tunneling microscopy, as well as modeling
144 dynamics of two-dimensional materials followed by electron microscopy. She received B.Sc. and
145 Ph.D. degrees in mechanical engineering from Hanyang University ERICA Campus, South Korea,
146 where she studied epitaxial growth of inorganic crystals on two-dimensional materials by electron
147 microscopy.

148
149 Shengpeng Huang is a Ph.D. student in the Nanoscale Science Department at the Max Planck
150 Institute for Solid State Research, currently working on single molecule analysis of RNA
151 structures. By combining electrospray ion beam deposition and scanning tunneling microscopy,
152 he deposited mass-selected RNA molecular ions on surfaces and imaged the RNA molecules
153 one-at-a-time to reveal their individual structures. He received his M.Sc. in Physics from the
154 University of Lund, Sweden, in 2023, where he studied structures and electronic properties of
155 bismuth islands grown on semiconductor surfaces using scanning tunneling microscopy and X-
156 ray photoelectron spectroscopy.

157
158 Kelvin Anggara is a group leader in the Nanoscale Science Department at the Max Planck Institute
159 for Solid State Research, working in the physical analytical chemistry of single molecules on
160 surfaces. He received his Ph.D. in physical chemistry from the University of Toronto, Canada, in
161 2018, and he did his postdoctoral stint as the Alexander von Humboldt fellow at the Max Planck
162 Institute for Solid State Research up until 2021. His research has been recognized by Karl
163 Freudenberg Prize, European Research Council Starting Grant, Human Frontier Science
164 Program Research Grant, among others.

165
166

167 **Dedications and acknowledgements**

168 We acknowledge support from ERC Project GlycoX (101075996) and Human Frontier Research
169 Program (RGEC31/2023), and we thank ACS and the ACS In Focus team, Tricia Louvar and Sara
170 Tenny, for this opportunity and for their support throughout the project. We acknowledge
171 proofreading support on our manuscript from Cynthia Khor and Lili Zhang.

172
173

174 **Chapter 1. What is electrospray ion beam deposition?**

175

176 **1.1. Introduction**

177

178 *“Break things and fix them”* is one of the tried and tested ways to learn how things work.

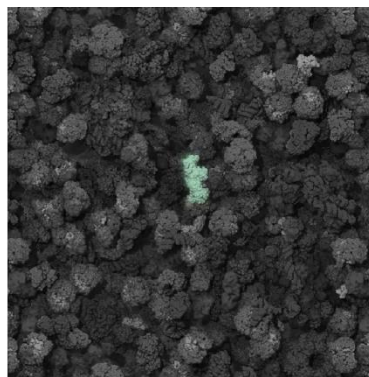
179

180 For example, to learn how computers work, you could pick up a screwdriver, take apart your
181 computer into its tiny components, and put them all back in a weekend.

182

183 But, have you wondered how you would go about learning how small systems — say, a cell —
184 work? Trillions of molecules, a few nanometers (10^{-9} meter) in size, from proteins to
185 carbohydrates, all *do something* to ensure the cell works as it should (Figure 1.1). Hidden within
186 these molecules are the answers to many important questions: How do our immune systems
187 work? Why and how cells turn cancerous? How do diseases emerge? Why do we age? The list
188 goes on.

189



190

191 **Figure 1.1 | A needle in a haystack.** Molecular crowding makes it difficult to understand how complex
192 systems work. The figure is a cartoon illustration of a single protein merely a few nanometers (10^{-9} m) in
193 size (highlighted in green) among many other biomolecules in a cell. Credit: Reproduced from McGuffee
194 SR, Elcock AH (2010) Diffusion, Crowding & Protein Stability in a Dynamic Molecular Model of the Bacterial

195 Cytoplasm. PLoS Comput Biol 6(3): e1000694. <https://doi.org/10.1371/journal.pcbi.1000694>. CC BY 4.0
196 <https://creativecommons.org/licenses/by/4.0/>

197

198 Cells are, of course, only one out of many complex systems that demand our thorough
199 understanding. Today, complex systems, ranging from sustainable materials that power our
200 civilization to catalysts that ensure our long-term food security, are all vital subjects in need of
201 investigation.

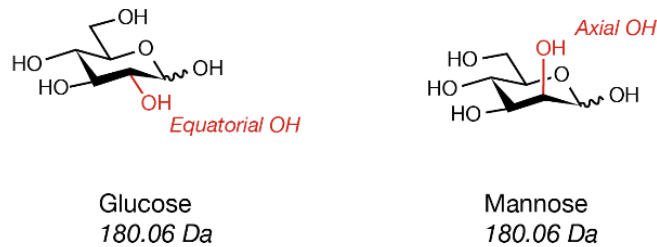
202

203 Clearly, one way to understand how a complex system works is to break it down to its individual
204 constituents, identify them, and understand how they work with one another to accomplish a task.
205 This means that first we need to *identify every single molecule* that makes up a complex system
206 – but how can we do this?

207

208 To answer this question, let us consider how these molecules differ. First, each of these molecules
209 can have a different molecular formula (i.e., the number of every type of atom in a molecule),
210 which gives each of them a specific molecular mass. For example, a cytochrome C protein
211 ($C_{558}H_{878}O_{155}N_{148}FeS_4$) has a mass of 12323.37 Da, while a glucose molecule ($C_6H_{12}O_6$) has a
212 mass of 180.06 Da. Second, while some molecules could have the same mass, they differ by how
213 each atom connects to one another. For example, glucose and mannose sugars ($C_6H_{12}O_6$) both
214 weigh 180.06 Da, with the only difference being that glucose has an equatorial OH while mannose
215 has an axial OH (Figure 1.2).

216



217

218 **Figure 1.2 | A molecule is a network of atoms.** Molecules with the same mass can be differentiated by
 219 how their constituent atoms connect to one another.

220

221 This brings us to two new problems: First, how can we separate molecules by their masses?
 222 Second, how can we determine the way atoms connect to one another in a molecule?

223

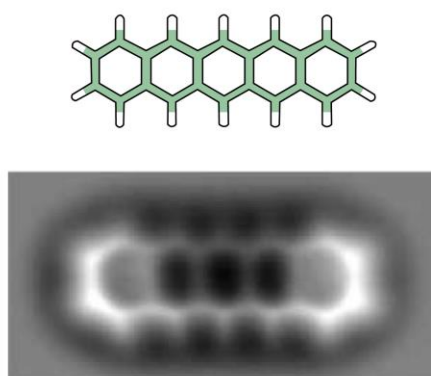
224 On the first problem, let us recall that the mass of an object dictates the magnitude of its
 225 acceleration when a force is applied to it. Imagine this: what happens if you kick an empty bottle
 226 versus the same bottle filled with water? Clearly, the empty bottle travels further than the filled
 227 bottle, because the lighter, empty bottle experiences a greater acceleration than the heavier, filled
 228 bottle. Hence, it follows that by applying an equal force (be that mechanical, electrical, magnetic,
 229 etc.) to a mixture of molecules, we could expect that molecules with different masses to move
 230 with different acceleration that subsequently separates them in space. However, to accomplish
 231 this, mass separation of molecules must be performed in a clean vacuum environment to
 232 eliminate friction effects caused by atmospheric gas molecules colliding with molecules we are
 233 interested in. To meet this requirement, a method to deliver molecules from solution phase into
 234 vacuum is thereby needed.

235

236 On the second problem, one simple solution toward observing the connections between atoms is
 237 to see individual chemical bonds directly in a single molecule – a stunning feat that has so far
 238 been accomplished only by scanning probe microscopy (SPM) (Figure 1.3). To attain such a

239 resolution, molecules need to sit on an atomically clean and flat surface at temperatures below
240 10 K (-263 °C); the latter is essential to remove any thermal motion of the molecule and to give
241 maximum stability to the microscope. The need for such a low temperature requires SPM imaging
242 to be conducted in an ultrahigh vacuum (UHV, $\sim 10^{-10}$ mbar) environment. This prerequisite
243 thereby calls for a method to transfer the intact molecules we are interested in from ambient
244 atmosphere onto an atomically clean surface in an UHV environment.

245



246

247 **Figure 1.3 | Atomically resolved imaging of a single molecule.** (Top) Model of pentacene molecular
248 structure. (Bottom) Direct observation of chemical bonds in a single pentacene molecule was accomplished
249 by scanning probe microscopy (SPM) at low temperatures (~ 4 K). Credit: From Leo Gross *et al.* The
250 Chemical Structure of a Molecule Resolved by Atomic Force Microscopy. *Science* **325**,1110-1114(2009).
251 DOI:[10.1126/science.1176210](https://doi.org/10.1126/science.1176210) Reprinted with permission from AAAS.

252

253 Here we showcase a technique that meets the aforementioned demands, termed electrospray
254 ion-beam deposition (ESIBD) (Figure 1.4). This technique enables single molecular species to be
255 isolated from a complex system for their structural studies on surfaces by microscopy techniques.

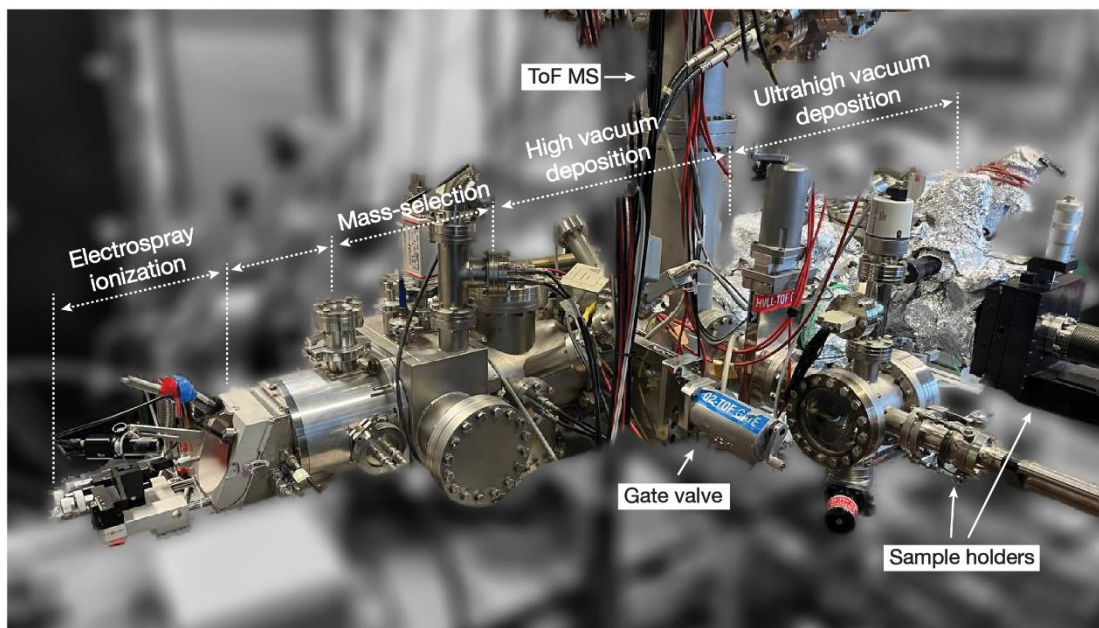
256 It accomplishes three important tasks:

257 (i) **Electrospray ionization:** delivery of molecules from solution to gas phase as ions;

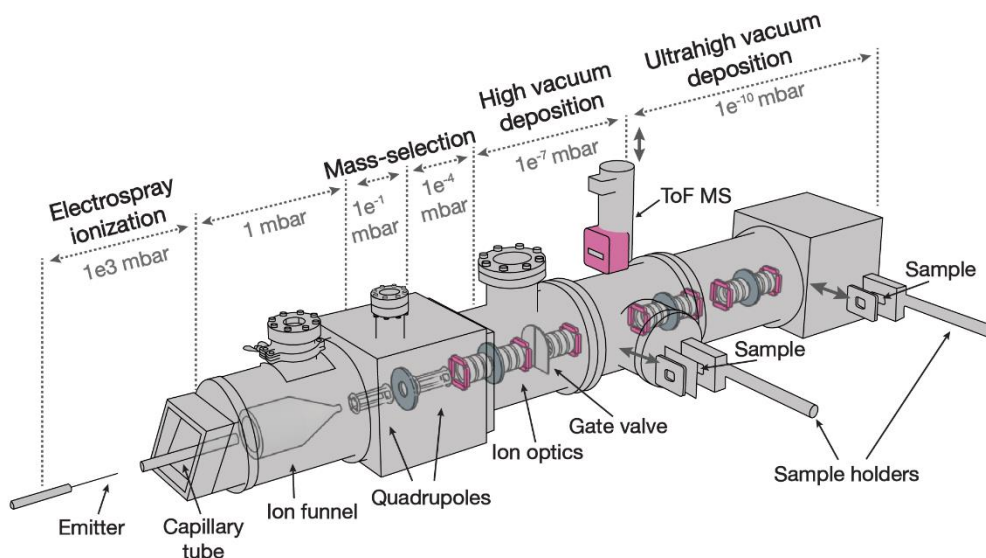
258 (ii) **Mass selection:** separation and selection of molecular ions by their mass; and

259 (iii) **Deposition:** soft landing of the mass-selected ions on surface for direct imaging.

a)



b)



261

262 **Figure 1.4 | Bringing molecules into vacuum.** (Top) Experimental apparatus and (Bottom) schematic of
 263 the electro spray ion beam deposition (ESIBD) technique highlighting the three aspects of the technique:
 264 electro spray ionization, mass selection, and deposition. The deposition can be done at different pressures
 265 (e.g., high vacuum and ultrahigh vacuum).

266

267 **Sidebar text box:** See the equipment in an actual lab! Click this link to view a video showing the instrument
268 set-up for electrospray ion beam deposition in a lab at the Max Planck Institute.
269 <https://www.youtube.com/watch?v=w-JBnzW6bdQ>

270
271 To show how the ESIBD technique contributes to existing fields of science, we highlight two
272 important applications of ESIBD (out of many in the literature): first, in enabling complex
273 molecules from cells to be observed and analyzed at the single molecule level, and second, in
274 enabling self-assembled structures from complex building blocks to be observed on surface. The
275 two applications discussed here demonstrate ESIBD as a valuable complementary addition to
276 present analytical workflows to determine the structure and interactions of complex molecules at
277 the ultimate single molecule level.

278

279 **1.2. ESIBD enables single molecule analysis of biomolecules**

280

281 The marriage of ESIBD to SPM allows any molecule that can be electrosprayed to be imaged and
282 structurally analyzed at the single molecule level on surface.

283

284 This approach is attractive for many complex molecules that remain intractable by today's
285 analytical technology, such as the dense sugar layer that covers cells (e.g., lipopolysaccharides
286 in bacteria, proteoglycans in human cells), the diverse RNAs that regulate the functions and
287 dysfunctions of our cells, the polymers central to our efforts to build a healthier and more
288 sustainable society (e.g., chitopolymers in biotechnology, marine polysaccharides in
289 environmental technology, and conjugated polymers in sustainable electronics and photovoltaics
290 technology), and many more.

291

292 Here, we will focus on one key application of ESIBD+SPM technique in analyzing biomolecules
293 decorated with glycans (also known as carbohydrates, oligosaccharides, or sugars) at the single
294 molecule level.

295

296 At this point, you may wonder: why should we care about glycans at all?

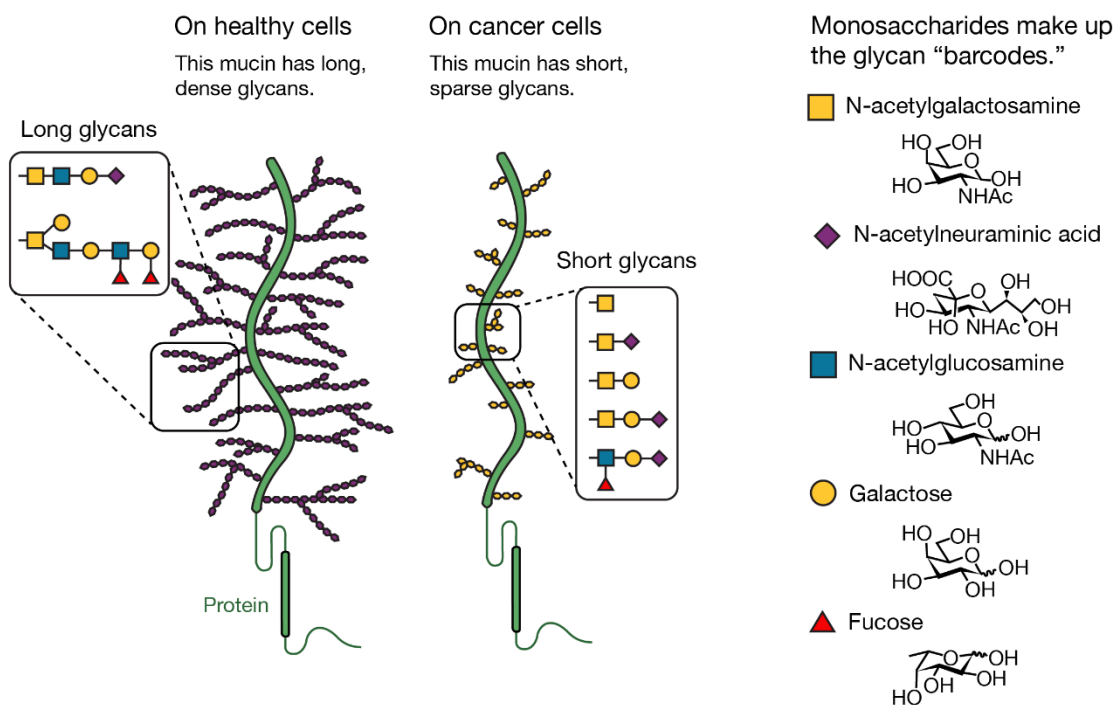
297

298 Glycans are one of the most understudied biomolecules, and yet the most ubiquitous ones in all
299 living systems. All cells without exception are covered with a thick layer of glycan molecules on
300 their surfaces that function like an ID card; they identify the type (e.g., human or bacterial) as well
301 as the state of the cells (e.g., healthy or cancerous). The latter is particularly valuable as it
302 presents an opportunity to detect cancerous cells simply by detecting specific glycans on cell
303 surfaces, potentially enabling early cancer detection. Such early detections are highly desired as
304 they increase the survival rates of cancer patients (late detection of cancer is associated with
305 fatalities).

306

307 As an example, mucins are a family of bottlebrush-like molecules found on cell surfaces, each
308 consisting of a protein chain decorated with glycans (Figure 1.5). These mucin molecules appear
309 differently in healthy cells than in cancerous cells. In healthy cells, mucins are densely decorated
310 with long glycans, while in cancerous cells, mucins are sparsely decorated with short glycans. In
311 every mucin molecule, the position and structure of every glycan along the protein chain is thought
312 to form a “barcode” that stores information that is so far readable only to biological systems – but
313 not us. Hidden within these barcodes are the answers to how biological systems recognize each
314 other, how our immunity works, how we achieve early cancer detection, and many more.

315



316

317 **Figure 1.5 | Mucin molecules in healthy and cancerous cells.** Mucins consist of a protein chain

318 decorated by glycans, which are long and dense in healthy cells but short and sparse in cancerous cells.

319 Examples of glycans present in mucins are given in the inset.

320

321 Now, given the immense value of mucins to our understanding of biology and to our therapeutics

322 development, the question is: what stops us from reading the barcode in every mucin present in

323 a cell?

324

325 The answer is technology. The technology available to us today to determine molecular structures

326 (e.g., mass spectrometry or cryo-electron microscopy) relies heavily on averaging structural

327 information obtained from millions of molecules (also known as ensemble averaging). This

328 approach is highly incompatible for mucins, given that a single cell possesses a large variety of

329 mucin molecules whose individual barcodes vastly differ from one another. As a result, ensemble-

348

349 Figure 1.6 shows this very direct imaging of a single mucin molecule. This direct imaging reveals
350 the protein chain of mucin (dashed line in Figure 1.6) and the *locations* where every glycan
351 connects to the protein chain (marked by red circles in Figure 1.6). Not only that, but direct imaging
352 also reveals the *structure* of every glycan attached to the protein chain, whether they are
353 trisaccharides or tetrasaccharides. Both information—the location and structure of the glycans—
354 unveils the barcode of the mucin (inset in Figure 1.6). By further imaging multiple mucin molecules
355 on surface, a collection of mucin barcodes emerges, revealing the diversity of unique mucin
356 barcodes as well as their relative composition – all at the ultimate single molecule level.

357

358 The success of the ESIBD+SPM technique in accessing individual mucin barcodes unlocks new
359 opportunities to study the true diversity of mucin barcodes in healthy and cancerous cells. Such
360 studies are anticipated to reveal the mucin barcodes that appear most often in healthy cells, but
361 not in cancerous cells, and vice versa, thus defining the most sensible mucin barcode targets for
362 pharmaceutical developments and therapeutic interventions.

363

364 **Sidebar text box:** Enhancing SPM imaging for biomolecular analysis. While SPM imaging triumphs in
365 accessing structural information at the single molecule level that is so far inaccessible to present analytical
366 techniques (e.g., mass spectrometry, ion mobility spectrometry, cryo-IR gas phase spectroscopy), SPM
367 imaging still has to improve before it could become a practical analytical tool to analyze glycan-containing
368 biomolecules (or any biomolecules in general). For instance, SPM sensitivity should be increased (e.g.,
369 using functionalized tip or using bias spectroscopy) to allow glycan isomers to be distinguished down to the
370 atomic level, or SPM imaging and analysis should be automated as much as possible to improve the data
371 throughput of the method.

372

373 **1.3. ESIBD enables preparation of self-assembled nanostructures on surface**

374

375 Beyond single molecule analysis, the ESIBD technique enables preparation of nanostructures on
376 surfaces. This is accomplished by depositing the mass-selected building blocks at a surface for
377 them to self-assemble into a functional material, allowing one to study how the building blocks
378 interact with one another and what the properties of the resulting material are at the atomic scale.

379
380 The ESIBD technique is attractive in its potential to access new materials on surface via a vast
381 choice of building blocks. The diverse electrospray-generated building blocks at our disposal and
382 the freedom to specify the sequence in which we use them allow us to embark upon a journey to
383 build new and specific materials with tailored properties.

384
385 This section summarizes one key achievement of the ESIBD technique in preparing two
386 dimensional (2D) materials using mass-selected ions.

387
388 But why? Why do we need to care about 2D materials? What is so remarkable about them?

389
390 New materials enable new wonders. New materials enable better lives. Before concrete, towering
391 skyscrapers were a mere dream. Before semiconductors, many electronic marvels that make our
392 lives more comfortable and connected (think the internet!) would not exist. New materials have
393 the power to revolutionize many aspects of our daily lives, shaping a better future for us.

394
395 Recent years have seen surging interests into a class of materials called 2D materials. Simply
396 put, they are layered materials that are only few atoms thick, such as graphene – a one-atom-
397 thick layer of carbon atoms arranged in a honeycomb pattern – or molybdenum disulfide (MoS_2)
398 – a three-atom-thick layer of sulfur and molybdenum atoms arranged in a triangular pattern.

399

400 What makes 2D materials so attractive? One answer is that they exhibit rich quantum properties
401 that are ripe for exploration and exploitation. These rich quantum properties result from electrons
402 in 2D materials being confined to a remarkably small thickness (i.e., few atoms thick), causing the
403 electrons to behave very differently when compared to electrons in bulk (3D) materials. One
404 consequence of this confinement is that electron energies now depend on the shape and
405 dimensions of the materials. This unlocks vast opportunities to engineer material properties by
406 simply changing their geometries. One historic example is the emergence of superconductivity
407 (i.e., the ability to conduct electricity without energy loss) when two layers of graphene are brought
408 together at a specific “magic” twist angle of 1.1 degree. Until today, no superconductivity has been
409 observed from a single layer of graphene or bulk carbon-based materials.

410

411 Despite the exciting discoveries and technologies that are emerging from the field of 2D materials,
412 their studies are inherently limited by the choice of 2D materials accessible by today’s preparation
413 methods, particularly in bottom-up preparation (where materials are built from their smaller
414 building blocks). Building blocks used to prepare 2D materials at a surface are often limited to
415 atoms or simple molecules that could withstand high temperatures, as they need to be thermally
416 evaporated onto the surface. As an example, organic molecules, such as sugars, could no longer
417 be used as building blocks as they would caramelize and burn when heated too strongly. The
418 restrictions in the choice of building blocks ultimately limits the versatility of 2D materials that could
419 be prepared on surface, thus creating barriers in exploiting the full potential of 2D materials in
420 addressing our societal challenges.

421

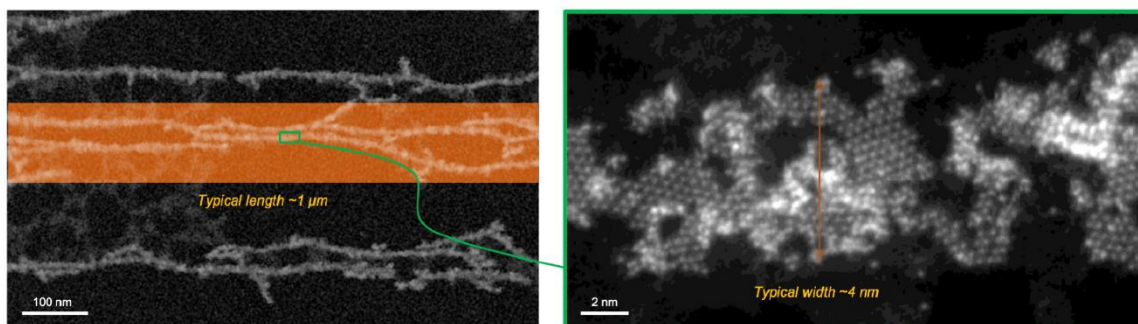
422 This is where ESIBD enters the picture.

423

424 The ESIBD technique expands the variety of building blocks that can be used to prepare materials
425 on surfaces to include thermally labile building blocks, such as inorganic clusters, organic

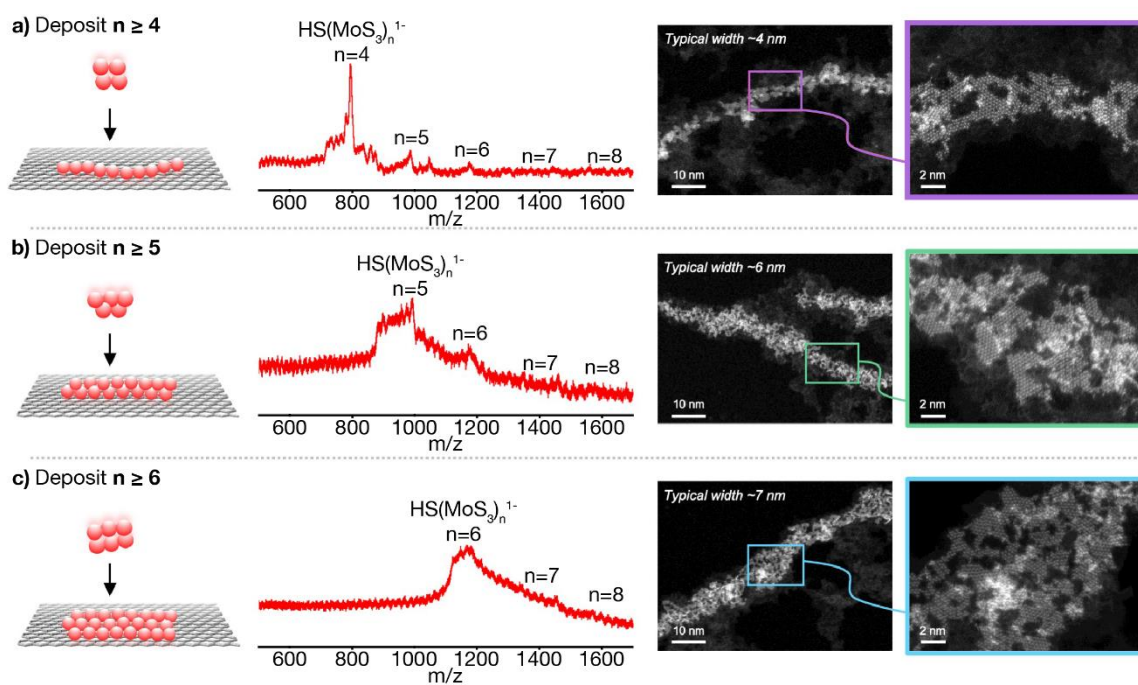
426 molecules, or even metal-organic frameworks. The ESIBD offers two advantages when compared
427 to material preparation based on thermal evaporation: (i) the electrospray ionization offers a
428 gentle transfer of complex, non-volatile molecules intact from solution into gas phase; and (ii) the
429 mass selection offers precise selection of building blocks deposited on surface. Both benefits
430 translate to a greater control of surface chemistry and thus unlocks access to a vast range of 2D
431 materials on surface.

432
433 In the following example, the ESIBD technique allows the use of MoS clusters to prepare MoS₂
434 nanoribbons, which are inaccessible by preparation techniques based on thermal evaporation.
435 These nanoribbons were visualized at the atomic level by scanning transmission electron
436 microscopy (STEM) to be few micrometers in length and few nanometers in width (Figure 1.7).
437



438
439 **Figure 1.7 | Nanoribbons of molybdenum disulfides prepared by the ESIBD technique.** MoS₂
440 nanoribbons (white strips) on graphene prepared by the ESIBD technique are visualized at the atomic scale
441 using scanning transmission electron microscopy (STEM). Credit: Reproduced from X. Zhang, V. Srot, X.
442 Wu, K. Kern, P. A. van Aken, K. Anggara, Controlled Formation of Nanoribbons and Their Heterostructures
443 via Assembly of Mass-Selected Inorganic Ions. *Adv. Mater.* 2024, 36,
444 2310817. <https://doi.org/10.1002/adma.202310817>. CC BY 4.0
445 <https://creativecommons.org/licenses/by/4.0/>
446

447 The power of ESIBD technique is further demonstrated by the precise selection of building blocks
 448 in fine tuning the final nanostructures on surface. In this example, MoS₂ nanoribbons obtained by
 449 depositing small MoS cluster (HMo₄S₁₃¹⁻) were observed to be few nanometers thinner than that
 450 obtained by depositing large MoS cluster (HMo₆S₁₉¹⁻) (Figure 1.8). This observation showcases
 451 the advantage of precisely selecting and depositing building blocks on surface in finely tuning the
 452 kinetics and thermodynamics of the surface chemistry that ultimately yields the final
 453 nanostructures.
 454



455
 456 **Figure 1.8 | Final nanostructures depend on deposited building blocks.** Varying the deposited
 457 HS(MoS₃)_n¹⁻ ions: (a) for n ≥ 4, (b) for n ≥ 5, and (c) for n ≥ 6, results in an increase in the average width of
 458 the nanoribbons from 4.7 to 7.3 nm, respectively. Credit: Reproduced from X. Zhang, V. Srot, X. Wu, K.
 459 Kern, P. A. van Aken, K. Anggara, Controlled Formation of Nanoribbons and Their Heterostructures via
 460 Assembly of Mass-Selected Inorganic Ions. *Adv. Mater.* 2024, 36,
 461 2310817. <https://doi.org/10.1002/adma.202310817>. CC BY 4.0
 462 <https://creativecommons.org/licenses/by/4.0/>
 463

464 In the future, due to the diverse building blocks accessible through electrospray ionization starting
465 from biomolecules to inorganic clusters, the ESIBD technique is expected to be instrumental in
466 accessing biomaterials as well as metal-organic framework materials with the goal of advancing
467 our understanding in fields as diverse as photovoltaics, electronics, catalysis, and many more.

468 1.4 [INSIDER – how did you get started in the field?]

469

470 **1.5. ESIBD roadmap**

471

472 The two cases discussed highlights the diverse role of ESIBD as a preparative technology, first,
473 in preparing microscopy samples and, second, in preparing complex materials on surfaces. While
474 these achievements signal a promising start, more research efforts are needed to explore the full
475 exciting potential of such preparative technology. One could thus speculate the directions upon
476 which ESIBD could be improved.

477

478 **1.5.1. Ion transmission at atmosphere-vacuum interface**

479

480 Finding strategies to harvest as many ions as possible at the atmosphere-vacuum interface
481 (especially in the region between 1000 to 1 mbar) remains a barrier toward the full potential of
482 ESIBD technique. This is due to the fact that the motion of ions in this pressure regime is
483 significantly affected by the gas flow dynamics (e.g., laminar vs turbulent flow and shockwaves),
484 and is thus no longer predictable by simply calculating the forces exerted on the ions by electric
485 fields from electrodes (Note: in pressures below 10^{-4} mbar, the motion of ions are governed by
486 electric fields which simplify the design process of the ion steering and focusing elements). The
487 difficulty in predicting the ion motions often leads to challenges in designing the best atmosphere-
488 vacuum interface. Today, the best solution to this problem is the use of ion funnels which allows

489 ions to be transmitted into vacuum with an ion flow as high as few nA (nanoamperes). However,
490 more focused efforts are required to push this transmission limit of the ESIBD technology to
491 include molecules that are not known to ionize well.

492

493 **1.5.2. Selection of ion shape**

494

495 Given that two molecular ions with the same mass-to-charge ratio could have a different molecular
496 geometry (e.g., a protein that could have various folding states or a molecule that could have
497 various relative orientation among their functional groups), a profitable direction to develop the
498 ESIBD technique is to include a scheme to perform ion selection by its respective shape. The
499 principles to develop this are readily available from the sister field of gas phase ion mobility
500 spectrometry (IMS). In IMS, ions are separated by their shapes by letting the ion drift through a
501 chamber filled with inert gases with a constant electric field. Molecular ions with larger cross
502 section (e.g., a star-shaped molecule) tend to travel slower than molecular ions with smaller cross
503 section (e.g., a stick-shaped molecule).

504

505 **1.6. Next chapters**

506

507 The subsequent **Chapters 2 to 4** will further detail the ESIBD technique as follows:

508 **(i) Chapter 2 – Electrospray ionization.** Molecules are brought from solutions into vacuum as
509 molecular ions by using a technique termed “electrospray ionization.” Electrospray generates
510 micrometer-sized (10^{-6} m) droplets of the solutions that contain the molecules we are interested
511 in. These microdroplets are the source from which molecular ions are obtained.

512 **(ii) Chapter 3 – Mass selection.** The molecular ions are subsequently focused into a beam of
513 ions. This ion beam is subsequently transmitted to a mass selector which serves to transmit ions

514 with specific mass-to-charge ratio (m/z), effectively removing any unwanted ions from the ion
515 beam.

516 **(iii) Chapter 4 – Ion soft landing on surfaces.** The purified ion beam is aimed at a clean surface
517 for their surface deposition. Here the kinetic energy of incident ions is typically reduced to achieve
518 intact deposition, that is, soft landing, of the molecules on a surface for their single molecule
519 microscopy studies.

520

521 **1.7. Read these next**

522

523 **1. Effects of crowded molecular environment in living systems:** Diffusion, Crowding & Protein
524 Stability in a Dynamic Molecular Model of the Bacterial Cytoplasm. PLOS Computational Biology
525 6, e1000694 (2010).

526 **2. How to use SPM to visualize single chemical bonds in molecules:** The Chemical Structure
527 of a Molecule Resolved by Atomic Force Microscopy. Science 325, 1110 (2009).

528 **3. An example of how ESIBD enables analysis of single biomolecules:** Direct observation of
529 glycans bonded to proteins and lipids at the single-molecule level. Science 382, 219 (2023).

530 **4. An example of how ESIBD enables preparation of inorganic 2D materials:** Controlled
531 Formation of Nanoribbons and Their Heterostructures via Assembly of Mass-Selected Inorganic
532 Ions. Advanced Materials 36, 2310817 (2024).

533 **5. Detailed reviews describing the ion soft landing phenomena and instrumentation: (a)**
534 Collisions of ions with surfaces at chemically relevant energies: Instrumentation and phenomena.
535 Reviews of Scientific Instruments 72, 3149 (2001). **(b)** Mass Spectrometry as a Preparative Tool
536 for the Surface Science of Large Molecules 9, 473 (2016).

537 **6. Soft landing applications in synthesis of multilayer materials: (a)** From Isolated Ions to
538 Multilayer Functional Materials Using Ion Soft Landing. Angew. Chem. Int. Ed. 57, 16270 (2018).

539 **(b)** Chemical Synthesis with Gaseous Molecular Ions: Harvesting $[\text{B}_{12}\text{Br}_{11}\text{N}_2]^-$ from a Mass
540 Spectrometer. 62, e202308600 (2023).
541

542 Chapter 2. The electrospray ionization

543

544 2.1. Introduction: Giving wings to molecular elephants

545

546 **Sidebar text box:** Ionization strategies. Electrospray ionization (ESI) is one of the typical means to
547 generate ions in gas phase. Other than ESI, typical ion sources include electron impact (EI) ionization,
548 where electrons are collided at ~70 eV with molecules (M) to form positive molecular ions (M⁺); or matrix
549 assisted laser desorption ionization (MALDI), where lasers are used to ablate and desorb molecules
550 embedded in a matrix (usually aromatic acids) to give molecular ions at low charge states. We refer the
551 reader to literature for an exhaustive survey of ionization methods (Finkelstein, J. Development of ionization
552 methods. *Nat Methods* **12** (Suppl 1), 6–7 (2015). <https://doi.org/10.1038/nmeth.3538>; Hansell, C. Enter the
553 matrix. *Nat Methods* **12** (Suppl 1), 17 (2015). <https://doi.org/10.1038/nmeth.3527>; Dellisanti, C.
554 Electrospray makes molecular elephants fly. *Nat Methods* **12** (Suppl 1), 15 (2015).
555 <https://doi.org/10.1038/nmeth.3525>)

556

557 The ESIBD technique uses electrospray ionization (ESI) to reliably transfer macromolecules from
558 solution phase to gas phase. This chapter aims to present a mental model of the ESI process as
559 a starting point to help you see: (i) which factors are critical to ensure successful delivery of
560 molecules from solutions into the gas phase and (ii) what strategies are available at your disposal.

561

562 You may wonder at this point: Why electrospray? What is it? How does it work?

563

564 Before that, let us challenge you. Imagine some giant molecules (say, proteins) floating inside a
565 big pool of water. We want to pull them out of the water – so that we can study them. How would
566 you go about doing this?

567

568 Well, one way is to **disperse the solution into tiny droplets**. By doing so, we significantly reduce
569 the number of solvent molecules (here, water) for every protein molecule. The smaller we can

570 make these droplets, the less effort it will take to further remove these solvent molecules from the
571 droplets so that we end up with the solvent-free protein molecules we want.

572

573 This brings us to another problem: How can we make the tiniest droplet possible?

574

575 Think of a garden hose. You will notice that water exits the hose at a much higher speed if we
576 squeeze the opening of the hose. By squeezing it even further, the water can shoot out so quickly
577 that it breaks into droplets. The underlying physics is based on the continuity equation in fluid
578 dynamics, which states that for an incompressible liquid (such as water) the flow rate (volume per
579 time) entering the system (Q_{in}) must equal to the flow rate exiting it (Q_{out}).

$$Q_{in} = Q_{out} \quad (\text{Eq. 2.1})$$

580 Where the flow rate is defined as the flow speed (s) multiplied by the flow cross section area (A).

581 Modifying the exit flow rate (Q_{out}) with this expression gives us:

$$Q_{in} = (A_{out}) \cdot (s_{out}) \quad (\text{Eq. 2.2})$$

582 Accounting for the garden hose phenomena, this equation shows that, as we leave the tap open
583 the same way (constant Q_{in}), reduction in the hose opening ($A_{out} \downarrow$) causes water to exit the hose
584 at higher speed ($s_{out} \uparrow$).

585

586 One interesting consequence of fluid stream moving at high speed is that they break apart into
587 smaller droplets, as the kinetic energy of the fluid is able to overcome the cohesive force that
588 holds the liquid together. Hence, it follows that we need to dramatically reduce the opening
589 diameter of the nozzle down to molecular sizes. How can we do this within practical limits?

590

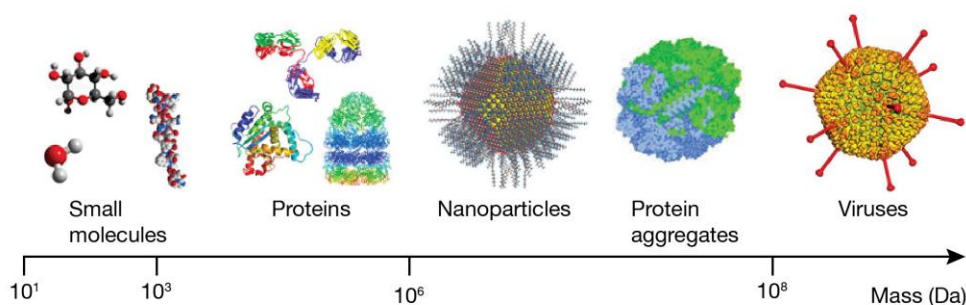
591 One idea is to use electric fields to shape the liquid itself into a nozzle-like cone shape.

592

593 This cone shape shrinks the diameter of the liquid stream down to hundreds of nanometers,
594 creating droplets whose sizes approach the sizes of macromolecules. This technique is called
595 **electrospray ionization (ESI)**, and it remains to be one of the most reliable methods to transfer
596 molecules from solutions into gas phase.

597
598 ESI offers two important advantages. First, many molecules have been demonstrated to be
599 amenable to ESI as long as they could exist as ions. As a result, ESI has become one of the
600 cornerstones of mass spectrometry, showing successful delivery of biological macromolecules
601 (e.g., protein complexes) up to intact viruses and microorganisms into the gas phase (Figure 2.1).
602 Second, ESI requires very little sample quantity, as low as 0.1 nanomoles (10^{-10} moles), making
603 it a highly valuable method to analyze samples available in trace quantity, such as biological
604 samples.

605



606
607 **Figure 2.1 | Analytes amenable to ESI: from small molecules to big viruses.** Examples of analytes
608 accessible by ESI, ranging from small molecules (a few Daltons) to viruses (a few Megadaltons). Credit:
609 Reproduced from Arnaud, C.H; Charge Detection Mass Spectrometry Measures molecular Structures Too
610 Big For Regular Mass Spec; C&EN. **2019**, 97 (36). Copyright 2019 American Chemical Society.

611
612 In the following sections, a model of the ESI process is presented to lay out all factors critical to
613 ensure successful delivery of molecules from solutions into gas phase. This includes discussion

614 on (i) how molecular ions emerge from the ESI-generated droplets, (ii) the choice of emitter
615 parameters, and (iii) sample solution parameters.

616

617 **2.2. How it works: From liquid jets to single ions**

618

619 The ESI process transfers molecules from sample solutions into the gas phase as molecular ions.

620 The process begins with the application of high voltages (above 0.5 kV) to a capillary filled with a

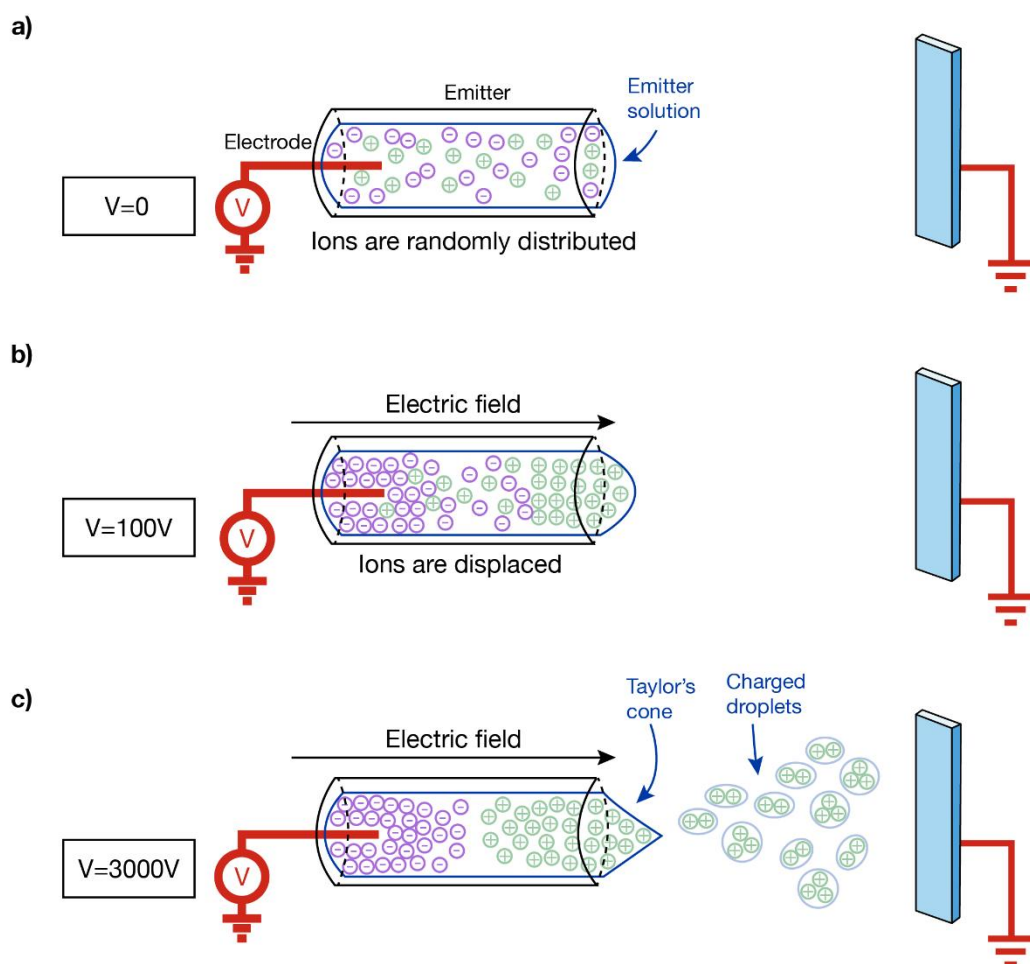
621 sample solution, known as an “emitter.” The applied voltage shapes the liquid at the end of the

622 emitter into a cone-like structure (known as Taylor cone) that eventually breaks apart at its apex

623 into sub-micrometer-sized charged droplets (Figure 2.2). These droplets continue to shrink and

624 disintegrate until single molecular ions are formed (Figure 2.3).

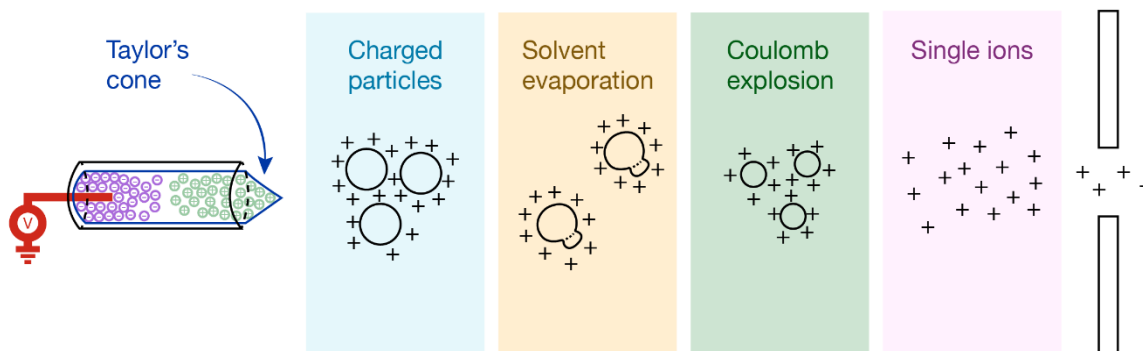
625



626

627 **Figure 2.2 | Sending molecules from solutions into gas phase.** ESI generates a stream of microdroplets
 628 from which molecular ions emerge. The example is shown here for ESI in positive mode, generating
 629 positively charged droplets which subsequently evolve into positively charged molecular ions. Negatively
 630 charged ions are generated when ESI is operated in negative mode.

631



632

633 **Figure 2.3 | Ion formation mechanism in electrospray ionization.** The electrospray ionization process
 634 develops from microdroplet formation to molecular ions in gas phase. Here we only show an example of
 635 positive ions, but negative ions can also be generated depending on the polarity of the high voltage applied
 636 to the emitter.

637

638 Now let us take a closer look into every step of the ESI process.

639

640 First, let us see how the Taylor cone is formed. By applying a voltage through an electrode to the
 641 sample solution, say, a positive voltage, negative ions in the solution are brought closer to the
 642 electrode while positive ions in the solution are repelled as far as possible from the electrode
 643 toward the emitter tip (Figure 2.2). As the applied voltage is increased, more positive ions would
 644 accumulate at the tip, and eventually above a certain voltage threshold, a stable Taylor cone is
 645 formed, generating from its cone apex, a stream of droplets containing positive ions. But wait,
 646 with the positive ions leaving the liquid, does this mean the solution becomes more and more
 647 negative in charge? No. The liquid stays charge neutral due to the redox reactions occurring at
 648 the electrode-liquid interface, either by producing positive ions (e.g., H_3O^+) to replenish the
 649 positive ions that left the liquid or by turning the negative ions into neutral molecules, depending
 650 on the solution composition. Note that while the mechanism here is described for ESI in the
 651 positive mode, the same mechanism applies to the ESI process in negative mode (where the
 652 applied voltage is negative), which generates droplets containing negative ions.

653

654 Now, let us follow the fate of the ions in the droplets after they have left the emitter (Figure 2.3).
655 In ESIBD, these droplets are delivered into vacuum via a heated tube. By heat convection, this
656 heated tube helps to evaporate the remaining solvent in these droplets. As more and more of the
657 solvent leaves the droplet, the droplet shrinks. The reduced droplet size brings the ions closer to
658 one another, causing the repulsive forces between ions to skyrocket. Eventually, below a critical
659 size, the repulsive forces between the ions are enough to overcome the surface tension of the
660 droplet, causing the droplet to disintegrate into smaller offspring droplets in a process called
661 “Coulomb fission.” The same evaporation-fission cycle continues for the offspring droplets.

662

663 Unfortunately, the mechanism of how molecular ions emerge in the final step of the ESI process
664 remains obscure due to the absence of direct experimental observation. Despite that, two models
665 have emerged from computational studies of the ESI process. The ion evaporation model (IEM)
666 proposes that ions are directly expelled from the shrinking droplets due to the increased repulsion
667 between ions, while the charge residue model (CRM) proposes that repeated evaporation-fission
668 cycles occur until one single molecular ion is left in every droplet, which further evaporates to yield
669 single molecular ions. A special intermediate case called chain ejection model (CEM) has also
670 been proposed to explain the ion formation mechanism of highly charged polymer ions. Our
671 understanding of the ESI process would benefit from more experiments investigating the
672 circumstances of the IEM, CEM, and CRM mechanisms.

673

674 Another mystery that calls for direct experimental observation is how Coulomb fission events
675 change the composition of the ions in the droplets, and how this composition differs from the ion
676 composition in the sample solution. As the droplets shrink to volumes that approach molecular
677 sizes, molecules in these droplets may behave differently from how they would behave in bulk
678 solutions. As a result, chemical equilibrium in such confined systems may differ radically from

679 chemical equilibrium in bulk solutions, leading to interesting phenomena that have only been very
680 recently reported in literature such as acceleration of reaction rates in microdroplets.

681

682 **2.3. ESI in practice**

683

684 The performance of ESI in delivering molecules from solutions into gas phase could be measured
685 by comparing how many ions arrive at a detector in vacuum (measured as ion current) to the
686 consumption rate of the sample solution. This so-called ESI efficiency is an important figure of
687 merit that assesses how well the ESI parameters work in delivering the molecules we are
688 interested in from solutions into gas phase.

689

690 For example, if we are interested in measuring the ESI efficiency of a sample solution containing
691 10^{-5} M of a dye molecule, first we need to convert the observed ion current from the intact molecule
692 (e.g., few picoamperes, 10^{-12} A) into the number of molecules arriving per unit time on the
693 detector. Assuming that an intact dye carries a charge of +2, the charge carried by a single dye
694 ion is thereby 3.2×10^{-19} C (= 2 × elementary charge), which gives us an arrival rate of around 3
695 million dye ions per second on our detector (obtained from dividing 10^{-12} A by 3.2×10^{-19} C). This
696 arrival rate could now be compared to the consumption rate of sample solution (e.g., few
697 nanoliters per minute). Given the concentration of 10^{-5} mol of dye molecules per liter, the total
698 number of molecules consumed by the ESI process is thereby 1.6×10^{-16} mol per second
699 (obtained from 10^{-5} M multiplied by 10^{-9} L/minute) – or around 100 million of molecules per second
700 (where 1 mol = 6.022×10^{23} molecules). Comparing the ion current (3 million molecules per
701 second) against the sample solution consumption rate (100 million molecules per second) brings
702 us to 3% ESI efficiency.

703

704 The ESI efficiency depends on many factors, such as the emitter, the flow rate, the structure of
705 analytes, the solvent, and many more. As these factors may lead to dramatic changes in
706 efficiency, this section aims to provide practical guidance to navigate the art of finding the best
707 parameters for a given analyte.

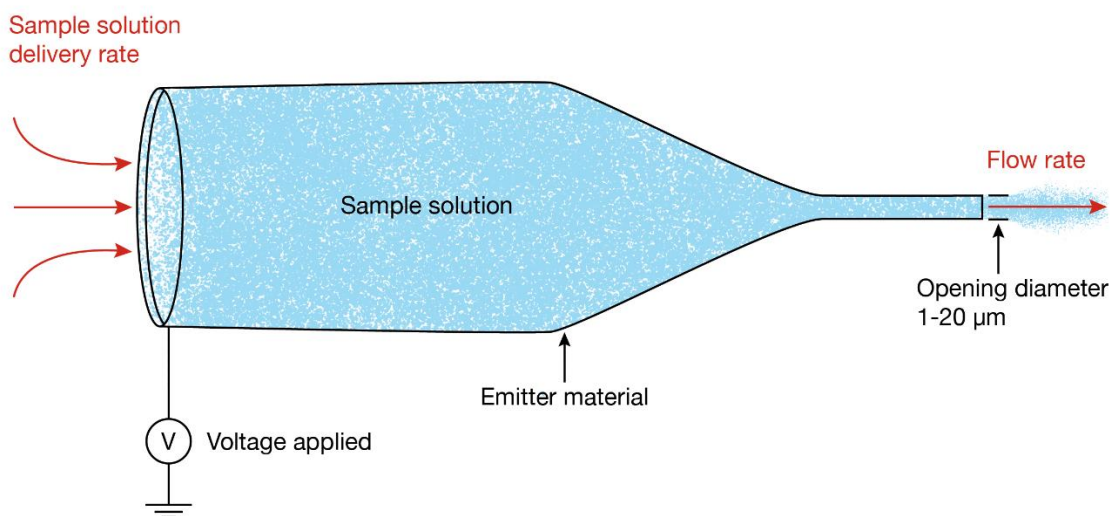
708

709 2.3.1. The emitter

710

711 First, let us discuss critical parameters in the ESI emitter, such as the material, the opening
712 diameter, and the flow rate, as well as how these affect the ESI efficiency (Figure 2.4).

713



714

715 **Figure 2.4 | Important parameters in an ESI emitter.** ESI efficiency depends on the emitter material, the
716 opening diameter, and the flow rate.

717

718 An ESI emitter can be made of many different materials, such as metal, glass, plastic, or even
719 paper! Metallic emitters offer long lifetime and reusability; but they may be challenging to fabricate,
720 especially in achieving small opening diameter (around 20 μm or smaller), and hence they are
721 more often used for ESI at high flow rates (around few μL per minute). Nonmetallic emitters are

722 more fragile, but are low cost and easy to fabricate, and thus are more often used for ESI at low
723 flow rates (around few nL per minute) which demands a very small opening diameter (around 1-
724 2 μm or smaller). To deliver high voltages to nonmetallic emitters, we can either (i) put an
725 electrochemically inert Pt wire in contact with the solution inside the emitter, or (ii) coat the emitter
726 with conductive metal (e.g., Pt).

727

728 Why should we care about flow rate? The flow rate is critical in ESI as it dictates the size of
729 droplets that come off the Taylor cone. Smaller droplets are thought to undergo less Coulomb
730 fission cycles, causing a higher proportion of molecules from the sample solution to end up as
731 molecular ions. Simply put, low flow rate gives smaller droplets – and smaller droplets give higher
732 ESI efficiency.

733

734 Here are two common ways to get low flow rates: by lowering the solution delivery rate to the
735 emitter; and by reducing the opening diameter of the emitter. First, in the case of *online* ESI where
736 sample solution is constantly fed to the emitter by external forces, such as a syringe pump or a
737 back-pressure, a low flow rate is obtained by lowering the pump speed of the syringe pump or
738 lowering the gas pressure that pushes the sample solution toward the emitter tip. In the case of
739 *offline* ESI where sample solutions are drawn from the emitter tip solely due to the electric field,
740 the flow rate is already at the minimum. A further strategy to reduce the flow rate is to reduce the
741 emitter opening diameter to few μm or lower. This is known to reduce the flow rates to as low as
742 few nanoliters per minute.

743

744 While all presented strategies are known to increase ESI efficiency, care must be taken in
745 practice. For example, a smaller opening diameter of an emitter makes it more prone to clogging,
746 thus making long unsupervised ESI sessions unfeasible. Also, lowering the sample solution
747 delivery rate may decrease the total ion current observed as the ESI efficiency may have reached

748 100% and the ion current is now bottlenecked by the amount of molecular analyte introduced to
749 the Taylor cone.

750
751 However, one important benefit in reducing the opening diameter of an emitter is the reduction of
752 threshold voltage needed to form a stable Taylor cone. An emitter with a few μm opening needs
753 0.5 to 1 kV to obtain a stable Taylor cone, while an emitter with a few tens of μm opening needs
754 3 to 4 kV. Low threshold voltage is highly beneficial to reactive and fragile molecules in sample
755 solutions as it reduces the electrochemical contamination of the sample solution as well as the
756 fragmentation of molecules in the sample solution, thereby increasing the amount of analytes
757 delivered into the gas phase as ions.

758

759 **2.3.2. The sample solution**

760

761 Apart from the emitter parameters, we can also play around with the sample solution parameters.
762 Here we present strategies on how to optimize them.

763

764 One way to approach this problem is to first look at the chemical structure of molecule we would
765 like to bring to the gas phase – and ask ourselves: “What ion species do I want to observe in the
766 gas phase?”

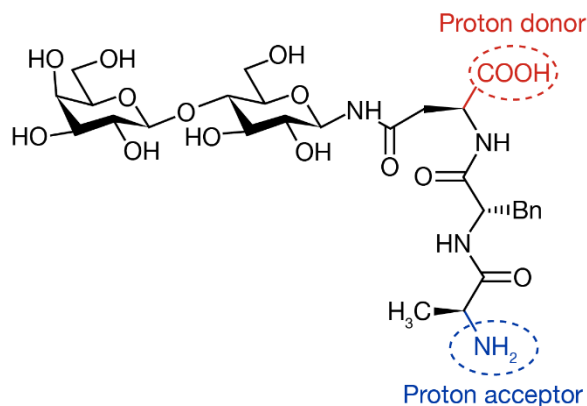
767

768 Before we answer this, it is useful to know two classes of ions accessible by ESI: bare ions and
769 adduct ions. For a given target atom/molecule (M), bare ions refer to M-ions without any additional
770 partner; while adduct ions refer to M-ions decorated with additional partner atoms or molecules.
771 Common bare ions are single ions (e.g., Rb^{+1} , Cs^{+1} , I^{-1} , Br^{-1} , etc.) and deprotonated molecules
772 (e.g., $[\text{M}-\text{H}]^{-1}$, $[\text{M}-2\text{H}]^{-2}$, etc. – these refer to singly and doubly deprotonated M molecule with -1

773 and -2 charge, respectively), whereas common adduct ions are protonated ions (e.g., $[M+H]^+$,
774 $[M+2H]^2$, etc. – these refer to singly and doubly protonated ions, respectively), ions decorated
775 with bare ions (e.g., $[M+Na]^+$, $[M+2Na]^2$, $[M+Cl]^-$, $[M+F]^-$ etc. – these refer to M molecule
776 decorated with 1 Na-ion, 2 Na-ions, 1 Cl-ion, and 1 F-ion, respectively), as well as hydrated ions
777 (e.g., $[M+H_2O]^+$, $[M+2H_2O]^+$, etc.).

778
779 Given the types of ions commonly accessible by ESI, we now need to examine what ions are
780 attainable from a given molecular structure. As an example, let us consider a glycopeptide
781 molecule (Figure 2.5). By inspecting the structure, we see that the molecule has a carboxylic acid
782 (RCOOH) group that could be deprotonated to give a $[M-H]^-$ ion as well as an amine (RNH_2)
783 group that could be protonated to give a $[M+H]^+$ ion. Could we also expect to see a $[M-H]^{2-}$ ion
784 as a result of deprotonation on both the RCOOH group (into a carboxylate, $RCOO^-$) and ROH
785 group (into an alkoxide, RO^-)? Not likely. The alcohol group (ROH) is a much weaker proton
786 donor than the carboxylic acid group (RCOOH), making the population of such doubly
787 deprotonated ions in solutions to be extremely small. As another example, let us consider a
788 protein, which may have many amine and carboxylic acid groups in a single molecule, say 10
789 COOHs and 10 NH_2 groups. The structure thereby implies that all NH_2 groups could be protonated
790 to give a $[M+10H]^{+10}$ ion or all COOH could be deprotonated to give a $[M-10H]^{-10}$, though ions with
791 incomplete protonation or deprotonation could also be expected, such as $[M-2H]^{2-}$ that comes
792 from the protein having 2 COOH groups deprotonated.

793



794

795 **Figure 2.5 | Planning the target ESI ion: an example glycopeptide molecule.** Ions of organic molecules
 796 obtainable from ESI are commonly dictated by the number of proton acceptors and proton donors in the
 797 molecule. Common proton donors are carboxylic acid groups (RCOOH), sulfate groups (ROSO₃H), and
 798 phosphates (ROPO₃H); while common proton acceptors are lone pair-containing groups, such as amines
 799 (RNH₂) and alcohols (ROH).

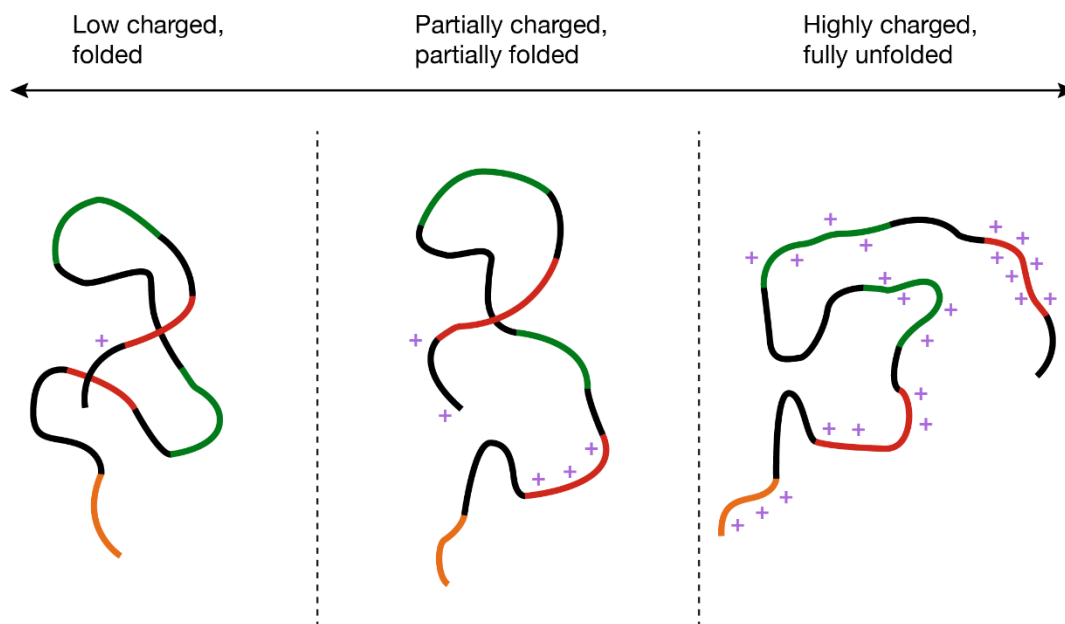
800

801 With all these choices, how would you decide which ions you should choose for ESIBD
 802 deposition? While the answer ultimately depends on the goal of your deposition experiment, we
 803 provide some important considerations based on ion composition and ion charge state. First, let
 804 us compare bare ions to adduct ions. Bare ions are preferred in analytical experiment (esp. when
 805 depositing unknown molecules) to remove as many contaminants as possible from the deposited
 806 molecules and allow the clearest interpretation of the deposited molecules from the single
 807 molecule imaging. On the other hand, adduct ions offer interesting possibilities to examine at the
 808 single molecule level the effect of adduct formation on the host molecule (e.g., the effect of
 809 hydration or sodium attachment on a molecule).

810

811 Next, let us consider the ion charge states (Figure 2.6). Ions with high charge states (e.g., protein
 812 at +10 charge state) are structurally unfolded as the charges repel each other to maximize the
 813 distance between them, whereas ions with low charge states (e.g., protein at +1 charge state) are

814 structurally folded, potentially retaining more structural similarity to their native structures in
815 solutions. In the context of SPM imaging studies, unfolded molecules on a surface are suitable
816 for sequence (primary structure) determination studies, whereas folded molecules on a surface
817 are suitable for 3D-structure (secondary structure) determination studies.
818



819
820 **Figure 2.6 | Unfolding polymer in gas phase by charge repulsion.** Molecules with low charge states
821 give folded structures, while molecules with high charge states give unfolded structures.
822

823 Once we define the target ions, we ought to provide the best conditions to increase their
824 population in sample solutions. Three common strategies are at our disposal: pH modification,
825 additives, and solvent. First, volatile acids or bases are often added to the sample solution to shift
826 the equilibrium in the solution toward the ions we desire. Common acids used to promote
827 protonated ions are formic acid (HCOOH), acetic acid (CH_3COOH), as well as trifluoroacetic acid
828 (CF_3COOH), while popular bases to promote deprotonated ions include ammonia (NH_3). Volatile
829 buffers are also commonly used to maintain a stable pH of the solution such that the native

830 structures of the molecules are preserved when isolated in the gas phase. Popular buffers include
831 ammonium acetate ($\text{NH}_4\text{CH}_3\text{COO}$) and ammonium bicarbonate (NH_4HCO_3). Next, additives are
832 often added to sample solutions to promote formation of adduct ions, such as adding sodium salts
833 (e.g., sodium formate, HCOONa) to promote formation of sodiated ions. Finally, solvent is a critical
834 parameter in sample solution. Less polar solvent with low surface tension promotes formation of
835 Taylor cone, generates smaller droplets, increasing the overall ESI efficiency. However, more
836 polar solvents improve stability of ions in the solution (recall that salt is soluble in water, a polar
837 solvent – but not in oil, a non-polar solvent, because the ions from salt are not well stabilized by
838 non-polar oil molecules). The delicate balance between these two factors leads to an empirical
839 list of common solvents used in ESI, such as 1:1 water:ethanol mix, methanol (CH_3OH), or
840 acetonitrile (CH_3CN). For hydrophobic analytes, organic solvents such as toluene ($\text{C}_6\text{H}_5\text{CH}_3$) have
841 seen success especially when mixed with methanol or acetonitrile. For biological molecules,
842 ammonium acetate buffer solution is often used to retain the folded structure of the biomolecules
843 from solution into gas phase.

844

845 **2.4. Read these next**

846

847 **1. Computational studies of ESI mechanism:** Unraveling the Mechanism of Electrospray
848 Ionization. *Anal. Chem.* 85, 2 (2013).

849 **2. Overview of chemical phenomena in microdroplets.** Reaction Acceleration in Electrospray
850 Droplets: Size, Distance, and Surfactant Effects. *J. Am. Soc. Mass Spectrom.* 30, 2022 (2019).

851 **3. Use of electrospray to study labile species in solution:** Evaluation of Electrospray Mass
852 Spectrometry as a Technique for Quantitative Analysis of Kinetically Labile Solution Species.
853 *Anal. Chem.* 71, 3785 (1999).

854

855 Chapter 3. The mass selection in vacuum

856

857 3.1. Introduction: Designing a filter for ions

858

859 From the previous chapter, we can see how we can send molecules from the solution into the gas
860 phase. Generally, however, the molecular ion beam that is generated from the electrospray
861 ionization process comprises a multitude of different molecular ionic species. To ultimately enable
862 single molecular imaging, we will require a method to select from this ion beam a single molecular
863 species of interest while simultaneously rejecting everything else. Typically, since we know the
864 masses of the molecules that we are interested in, we can filter the ions, keeping only those ions
865 that have the right masses. That is, **we want to mass select our molecules of interest.**

866

867 How do we go about filtering through all the molecules?

868

869 Well, since the molecules in our ion beam are charged, we can make use of a combination of
870 electromagnetic fields to do this filtering. This is because charged particles (either atoms or
871 molecules) respond in a particular way when exposed to these fields. As we will see later in this
872 chapter, these charged particles respond to these fields in a way that depends on their mass and
873 charge, or more specifically, their **mass-to-charge ratio** (m/z ; m = mass number, z = charge
874 number). The point is that with careful manipulation of these external fields, we can filter out,
875 based on their m/z values, unwanted molecules while keeping those that we care about in our ion
876 beam.

877

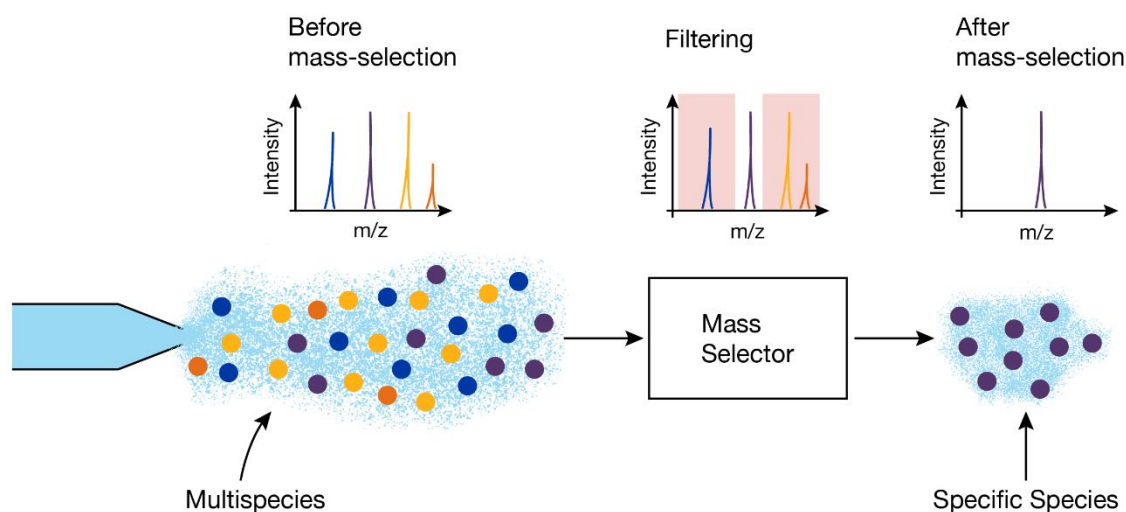
878 Sometimes, however, either by design or by chance, the molecules that we are interested in can
879 exist in our ion beam in different charged states. They could have a charge of +1, +2, +3, and so

880 on in the same ion beam. Despite having the same mass (since it is the same molecule) they will
881 have different m/z values, from their different charge states (same m different z). Thus, we can
882 also potentially choose the charge state of the mass-selected molecule of interest.

883

884 In the end, mass-selection means that we can have an ion beam that is **free of contaminants**
885 and that is **composed of a specific molecular species** that is **in a specific charged state**
886 (Figure 3.1).

887



888

889 **Figure 3.1 | Schematic of the mass-selection process.** The ion beam, generated from the electrospray
890 ionization process, may contain contaminants, multimolecular species, and/or molecules in multiple
891 charged states (e.g., +1, +2, +3, -1, etc.). Passing the ion beam through a mass-selector allows for the
892 purification of the ion beam by filtering out unwanted components, leaving us with an ion beam with a
893 specific molecule in a specific charged state.

894

895 To ensure reliability and robustness, even for weak ion beams, the mass selection is generally
896 performed under vacuum conditions (with pressures $\ll 1$ mbar). This ensures that ion trajectories
897 are determined and controlled solely by external electric and magnetic fields, which is critical for
898 precise mass-to-charge ratio selection. The ability to guide the ion beam into a mass-selector is

899 also crucial as otherwise nothing comes out from the mass selection process as nothing goes in
900 to begin with. Both aspects, establishing vacuum conditions and guiding ion beams, are discussed
901 in this chapter before finally discussing m/z mass-selection.

902

903 **3.2. Vacuum basics**

904

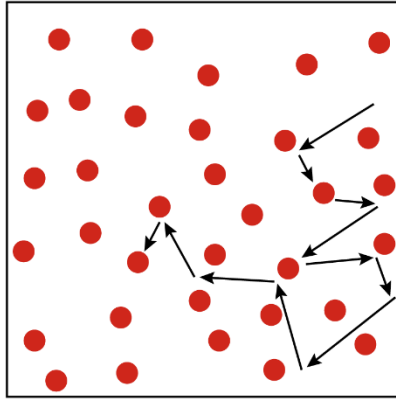
905 From the kinetic theory of gases, one can calculate the average distance that a molecule can
906 travel before colliding with other molecules. This average distance between successive collisions,
907 also known as the mean free path, necessarily depends on the pressure, which in turn depends
908 on the number of molecules in a given volume. In ambient pressure, the mean free path of
909 molecules is on the order of nanometers (see Table 3.1) whereas in pressures of $\sim 10^{-7}$ mbar, the
910 mean free path can reach kilometers. Under ultrahigh vacuum (pressures of $\sim 10^{-10}$), this mean
911 free path can reach hundreds of kilometers. What this means is that under ambient pressures,
912 the trajectory of one molecule is almost impossible to predict as it can undergo many collision
913 events in a short distance and time period. Under high to ultrahigh vacuum conditions, molecules
914 travel much farther without undergoing collisions, that is, their trajectories can remain unchanged
915 for much longer (except for when they hit the walls of the chamber they are confined to! See
916 Figure 3.2).

917

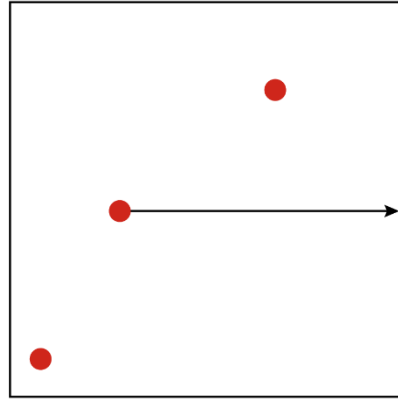
Pressure (mbar)	Mean free path
~ 1000 (ambient pressure)	~ 60 nm
~ 100 (low vacuum)	~ 10 μm
$\sim 10^{-2}$ (medium vacuum)	~ 10 mm
$\sim 10^{-7}$ (high vacuum)	~ 1 km
$\sim 10^{-10}$ (ultrahigh vacuum)	$\sim 10^3$ km

918 **Table 3.1 | Typical mean free path of particles in differing pressures at room temperature.**

a) High pressure:
Short mean free path



b) Low pressure:
Long mean free path



920

921 **Figure 3.2 | Mean free paths of particles in differing pressures.** Particles in high pressure regimes
 922 undergo frequent collisions with each other and therefore acquire a short mean free path. Whereas particles
 923 in a low-pressure regime rarely undergo collisions and acquire a long mean free path.

924

925 In essence, under high and ultrahigh vacuum conditions, one can treat particles as isolated
 926 objects free from influence from other particles. This has several advantages: (1) the analysis of
 927 the trajectories of charged particles in vacuum due to external electric and/or magnetic fields is
 928 made easier as collisions between particles (which affect the trajectories of the particles) can be
 929 reasonably ignored; (2) higher ion transmissions (e.g., through required apertures) can be
 930 achieved due to the severe reduction in random particle collisions that would alter ion trajectories;
 931 (3) unwanted chemical reactions between particles (due to collisions) can be controlled and
 932 severely mitigated; and (4) the breakdown voltage between two conductive electrodes in vacuum
 933 can be made very high (see Paschen's law).

934

935 **Sidebar text box:** What is Paschen's Law? Paschen's Law describes the relationship between the
 936 breakdown voltage required to initiate electrical discharge (such as a spark) between two electrodes. The
 937 law shows that for a given gas and electrode material, the breakdown voltage depends on the gas pressure
 938 and the separation between the electrodes. The breakdown voltage increases as the pressure decreases

939 well below ambient pressures. At lower pressures, the gas becomes less conductive because there are
940 fewer gas molecules to ionize to cause an electrical discharge between electrodes. However, discharge
941 can still occur even at lower pressures if the gap between the electrodes is sufficiently small.

942

943 **3.2.1. Establishing vacuum**

944

945 Creating a vacuum essentially means removing gas molecules from an enclosed environment to
946 reduce its pressure well below atmospheric pressure. In connection to high-vacuum or ultrahigh
947 vacuum single molecule imaging methods, stainless steel chambers (with polished clean interiors
948 so that little foreign contaminants can desorbed from surfaces) are employed as a vessel from
949 which air will be evacuated. Various kinds of vacuum pumps can then be connected to these
950 chambers to pump out internal gas and achieve the desired pressures. These vacuum pumps
951 can be broadly categorized into: (1) positive displacement pumps; (2) momentum transfer pumps;
952 and (3) entrapment pumps.

953

954 Positive displacement pumps work by mechanically trapping and expelling gas molecules to
955 reduce the pressure of the chamber. These kinds of pumps include rotary vane pumps, scroll
956 pumps and diaphragm/membrane pumps. These pumps are commonly used to achieve low to
957 medium vacuum (1 mbar to $\sim 10^{-3}$ mbar) within a chamber. Scroll and diaphragm pumps are also
958 often used as a backing pump (see below).

959

960 Momentum transfer pumps rely on high-speed motion to direct gas molecules out of the chamber.
961 A popular example includes turbomolecular pumps which are extremely effective for achieving
962 high to ultrahigh vacuum pressures (10^{-3} mbar to 10^{-10} mbar). These pumps however require
963 backing pumps to ensure that forevacuum level, that is the pressure level at the exhaust of the

964 turbomolecular pump, remains low (1 mbar to $\sim 10^{-3}$ mbar) to effectively maintain the high to
965 ultrahigh vacuum conditions in the chamber.

966
967 Entrapment pumps are pumps that capture gaseous molecules by condensing or chemically
968 binding them. Such pumps include cryopumps which can achieve high to ultrahigh vacuum by
969 trapping gas on cold surfaces as well as getter pumps which uses reactive materials to chemically
970 absorb gas.

971
972 While the kinds of pumps are an important factor to consider in establishing vacuum, other factors
973 to note are the pumping speed of the pump, e.g., turbomolecular pumps can come in small or
974 large sizes with small turbomolecular pumps expelling air at a lower rate than larger
975 turbomolecular pumps which can expel air at a higher rate. The size of the chamber that needs
976 to be pumped is also an important consideration. Smaller chambers can achieve a lower vacuum
977 level compared to a larger chamber, assuming both are pumped with an identical pump. Chamber
978 leaks can also limit the ultimate vacuum level that can be achieved. It is important to ensure that
979 the chamber is vacuum sealed correctly, i.e., no leaks are present. However, there are cases
980 where intentional leaks are introduced (see next section) which therefore must be considered
981 when establishing the appropriate vacuum level.

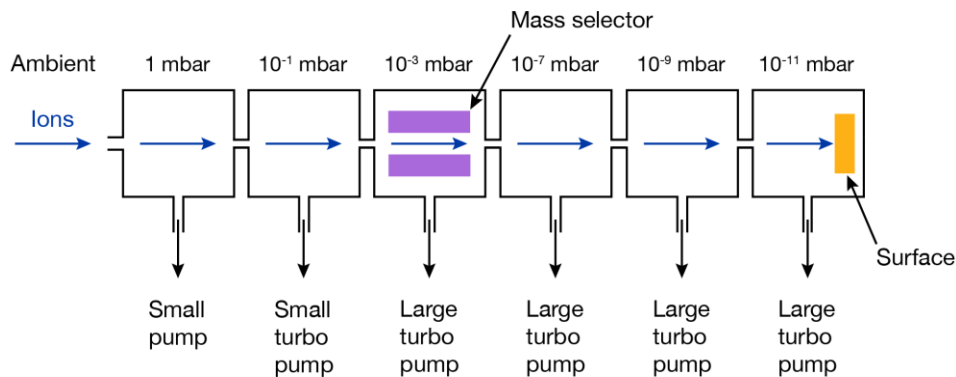
982 983 **3.2.2. Differential pumping**

984
985 The electrospray ionization process which transfers molecules in solution to gas phase happens
986 typically in ambient conditions. On the other hand, mass selection, surface deposition, and single
987 molecule imaging (e.g., with scanning tunneling microscopy or transmission electron microscopy)
988 are performed in a chamber under vacuum. We therefore need a way to bridge these two extreme

989 pressure regimes without severely compromising the vacuum integrity of the chamber. We
990 achieve this by means of differential pumping which is a technique to maintain different pressure
991 levels in adjacent sections of a vacuum chamber system.

992
993 This approach involves dividing the vacuum system into separate regions with vacuum-tight
994 partitions, each evacuated by its own dedicated pump (Figure 3.3). Narrow apertures or small
995 orifices connect these regions (these act as intentional leaks between the regions), restricting the
996 flow of gas between them. The reduction in gas flow between the regions ensures that each region
997 can maintain its designated pressure level. This way, we can design a set-up such that one end
998 of the vacuum chamber system is opened to ambient air (where we can introduce the gas phase
999 ions from electro spray ionization process) and the other end of the vacuum chamber is held at
1000 ultrahigh vacuum for depositing these molecules on a surface, for example.

1001



1002

1003 **Figure 3.3 | Differentially pumped vacuum system.** This schematic shows six vacuum chambers that
1004 are each pumped by a dedicated vacuum pump and are connected to each other via a small orifice. The
1005 pressure levels in the vacuum chambers decrease from the leftmost chamber to the rightmost chamber.
1006 The leftmost chamber has an opening to ambient air. This enables the introduction of ions from the
1007 electro spray ionization process directly into vacuum from low to ultrahigh vacuum conditions.

1008

1009 This differentially pumped chamber set-up maintains the vacuum integrity of each region while
1010 allowing for the feasibility of having an opening to ambient conditions as large as a few millimeters.
1011 This is not without its challenges as properly setting up a differentially pumped system requires
1012 precise engineering of the apertures between regions and pump placements to achieve the
1013 desired pressure gradient between the different regions. This also means increased system
1014 complexity and cost due to the need for multiple pumps. Despite these challenges, differential
1015 pumping is an indispensable tool enabling complex systems to operate across vastly different
1016 pressure ranges.

1017

1018 **3.3. Ion manipulation in vacuum**

1019

1020 For the purposes of mass-selection and surface deposition, it is essential that we can manipulate
1021 the trajectories of ions in vacuum. Proper trajectory control ensures that ions are guided efficiently
1022 through and between vacuum chambers, focusing them into narrow beams or directing them
1023 toward specific targets (e.g., a mass-selector or a surface). This helps to minimize any ion losses
1024 in the whole electrospray ionization beam deposition process. Additionally, trajectory
1025 manipulation compensates for initial ion dispersion, misalignment, or environmental disturbances,
1026 enabling accurate analysis or experimentation.

1027

1028 **3.3.1. Kinetic energies of ions**

1029

1030 The use of any electromagnetic fields to manipulate the trajectory of an ion invariably depends on
1031 how fast these ions are moving in vacuum, more specifically, it depends on their kinetic energies.
1032 When ions transit from a low-vacuum chamber ($\sim 10^{-1}$ mbar) into a high-vacuum ($\sim 10^{-3}$ mbar)
1033 chamber, the kinetic energy of these ions is largely determined by and somewhat proportional to

1034 the voltage (electric field) applied at the aperture between the chambers. In the low-vacuum
1035 chamber the mean free path of the ions, on the order of hundreds of micrometers, is significantly
1036 shorter than the dimensions of the chamber, which means ions can still undergo many collisions
1037 with residual gas molecules. The effect of these collisions results in the loss of the ions' kinetic
1038 energy until the ions acquire an average kinetic energy proportional to the temperature of the
1039 residual gas (as a mental model, note that it is difficult for a person to run through a crowded
1040 hallway and in fact, the person's speed is somewhat limited to the average speed of the crowd in
1041 that hallway).

1042

1043 Now, a weak DC electric field applied across the low-vacuum chamber to high-vacuum chamber
1044 interface helps ensure that the ions maintain enough momentum to transition effectively from the
1045 low-vacuum to the high-vacuum region. As ions enter the high-vacuum region, the mean free path
1046 of the ions increases dramatically, allowing the ions to travel unimpededly. Once in high-vacuum,
1047 the ions retain the kinetic energy imparted by that weak electric field as collisions with gas
1048 molecules in the high-vacuum regions are negligible.

1049

1050 **3.3.2. Electrostatic lenses (Einzel lenses)**

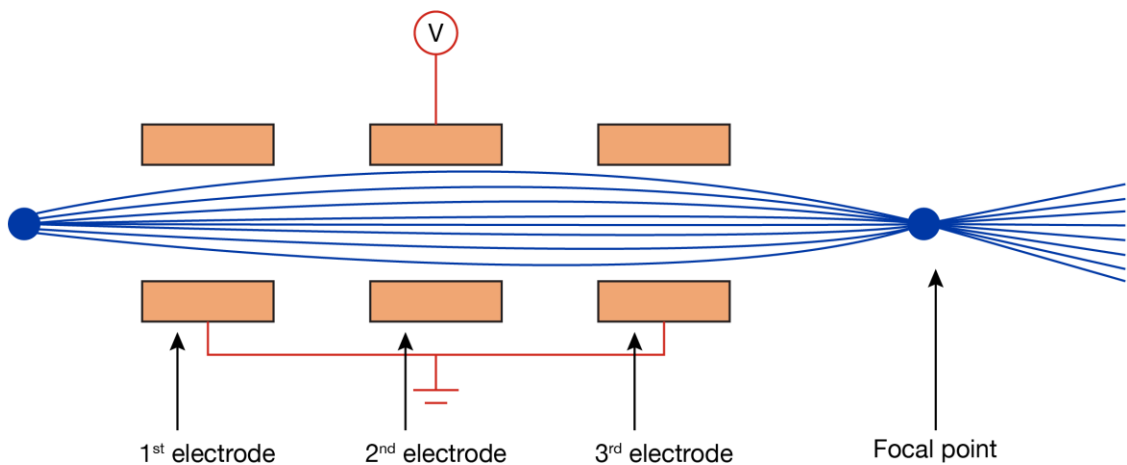
1051

1052 Einzel lenses are essential tools in ion optics for focusing ions without significantly altering their
1053 kinetic energy. They use electrostatic fields created by three cylindrical electrodes arranged
1054 coaxially along the ion's trajectory. The central electrode is usually held at a different electric
1055 potential than the two outer electrodes, allowing the lens to manipulate the trajectories of ions
1056 passing through them (Figure 3.4).

1057

1058 As an example, for a positively charged ion approaching the lens, the middle electrode is held at
1059 a higher electric potential compared to the two outer electrodes. As this positive ion enters the
1060 lens and exits the first electrode, it decelerates axially due to the increase in the electric potential
1061 (from the middle electrode) and is pushed outward radially. Upon entering the second electrode,
1062 the ion continues to decelerate axially (but at a slower rate) and is pulled radially inward. As the
1063 ion exits the second electrode, it starts to accelerate axially while still being pulled inward radially.
1064 As the ion enters the third electrode, its acceleration slows, and upon leaving the lens, the ion
1065 leaves with the same kinetic energy as it had before. As a result, an ion beam, depending on the
1066 applied potentials, can be focused into a tighter beam upon leaving the lenses. The point of focus
1067 of the ion beam (i.e., the focal point) can be adjusted by adjusting these potentials. Since the ion
1068 beam necessarily diverges beyond this point, successive Einzel lenses can be used to ensure
1069 that the ion beam is refocused.

1070



1071 **Figure 3.4 | Focusing ion beams with Einzel lenses.** The schematic shows a cross section of a three-
1072 electrode Einzel lens set-up. The outer two electrodes are held at the same potential, in this case they are
1073 grounded while the middle (second) electrode is held at a different potential. For a properly applied potential
1074 to the middle electrode, an ion beam entering the lenses can be made to focus to a focal point upon exiting
1075 the lenses.

1077

1078 While these lenses do not alter the kinetic energy of the ions passing through, the focusing effect
1079 of these lenses depends on the kinetic energy of these ions. Typically, ions with higher kinetic
1080 energy travel faster through the lenses and are less affected by the focusing field than those ions
1081 with a lower kinetic energy. For ions with higher kinetic energy, often higher potentials are needed
1082 to achieve the same degree of focusing. Tuning these potentials is therefore important to achieve
1083 the desired results. In fact, applying incorrect potentials can lead to ion beam divergence instead
1084 of convergence upon the ion beam leaving the lenses. In some scenarios, it is even possible to
1085 completely prevent ions from traversing the lenses resulting in a termination of the ion beam at
1086 the lenses itself.

1087

1088 If properly tuned, a series of these lenses placed along the intended ion beam path will ensure
1089 accurate guiding of the ion beam to its target and minimal loss in ion transmission throughout the
1090 vacuum chamber.

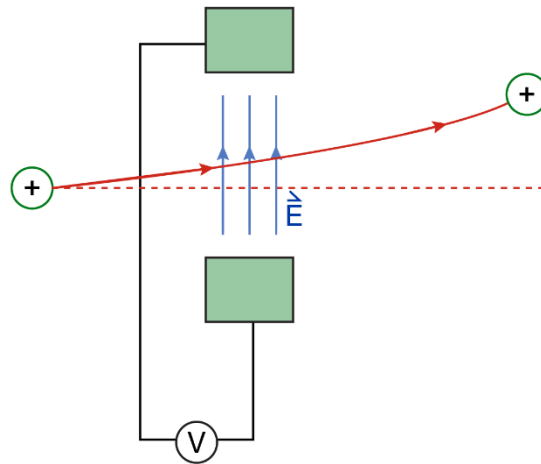
1091

1092 **3.3.3. Electrostatic steering plates**

1093

1094 Steering plates are pairs of parallel, flat electrodes used to deflect and align ion trajectories by
1095 creating uniform transverse electric fields relative to the ion beam path (Figure 3.5). Simply, two
1096 plates are placed on opposite sides of an ion beam. By applying a potential difference between the
1097 plates, a transverse electric field is generated which exerts a force on the ions (perpendicular to
1098 their motion), deflecting them toward the desired direction. The degree of deflection depends on
1099 the ion's charge, mass, velocity as well as the electric field strength. Having two additional plates
1100 in along the other axis provides for fine adjustments of the ion beam trajectory in the up-down or
1101 left-right axes. These steering plates can be used to correct for misalignments or to direct ions
1102 into the narrow apertures connecting multi-chamber vacuum systems.

1103



1104

1105 **Figure 3.5 | Ion deflection with steering plates.** The schematic shows a sideview of how a positively
1106 charged ion's trajectory can be deflected upwards (relative to unperturbed trajectory; red dashed line) by
1107 applying an electric field between the two electrodes (green).

1108

1109 3.4. Quadrupole mass selection

1110

1111 While there are different ways to perform mass selection—such as with a double focusing mass
1112 selector—a popular method for mass selection, especially in the context of soft landing, involves
1113 the use of a quadrupole mass selector. Its relatively low cost, straightforward design and ease of
1114 use make the quadrupole mass selector often a preferred choice in many circumstances. To this
1115 end, we focus on their principles of operation in this section. We note that the results of the mass
1116 selection process are often then checked with mass analyzers such as time-of-flight mass
1117 spectrometers, orbitraps, or Fourier transform ion cyclotrons, to name a few. The operating
1118 principles of these mass analyzers are not covered here but can be reviewed in the further
1119 readings section at the end of this chapter.

1120

1121 **3.4.1. m/z mass selection: how does it work?**

1122

1123 In general, mass selection based on the mass-to-charge ratio, m/z , of molecules depends on the
1124 combination of two physical laws. The first is Newton's Second Law (Eq. 3.1):

$$\mathbf{F} = m\mathbf{a} \quad (\text{Eq. 3.1})$$

1125 \mathbf{F} is force that an object of mass (m) requires to move it with some acceleration (\mathbf{a}). The second
1126 law is the Lorentz Force Law (Eq. 3.2):

$$\mathbf{F} = z(\mathbf{E} + \mathbf{v} \times \mathbf{B}) \quad (\text{Eq. 3.2})$$

1127 This law says that a particle with some charge (z) when exposed to some electric field (\mathbf{E}) and
1128 some magnetic field (\mathbf{B}) experiences a force (\mathbf{F}), on it that: (1) is proportional to the electric field
1129 (\mathbf{E}); and (2) is proportional to the cross product of the particle's velocity (\mathbf{v}), with the applied
1130 magnetic field (\mathbf{B}).

1131

1132 If we now substitute Eq. 3.1 into Eq. 3.2, and for simplicity we set $\mathbf{B} = 0$, we get:

$$\mathbf{a} = \frac{\mathbf{E}}{m/z} \quad (\text{Eq. 3.3})$$

1133 That is, if we know at some point in time that a particle with mass, m , charge, z , is travelling with
1134 velocity, \mathbf{v} , and it is exposed to some electric fields (\mathbf{E}), then we can use Eq. 3.3 to figure out the
1135 particle's trajectory for future times. The heart of mass selection comes from the fact that the
1136 trajectory of the particle depends, with all else being equal, on its mass-to-charge ratio (m/z) as
1137 seen in the denominator on the right-hand side of Eq. 3.3. If we are deliberate and creative with
1138 our choices for \mathbf{E} , we can get only molecules with the desired m/z to move through a defined path
1139 while forbidding other molecules with different m/z moving along that same path. Simply put, this
1140 is all the physics we need to build an ion filter with electric fields. We say creative, as we are not
1141 restricted to using just *static* or constant fields, as Eq. 3.3 is also valid for time-dependent and
1142 space-varying fields $\mathbf{E}(\mathbf{r}, t)$, which can give rise to non-trivial particle trajectories.

1143

1144 **3.4.2. Quadrupole arrangement and principles**

1145

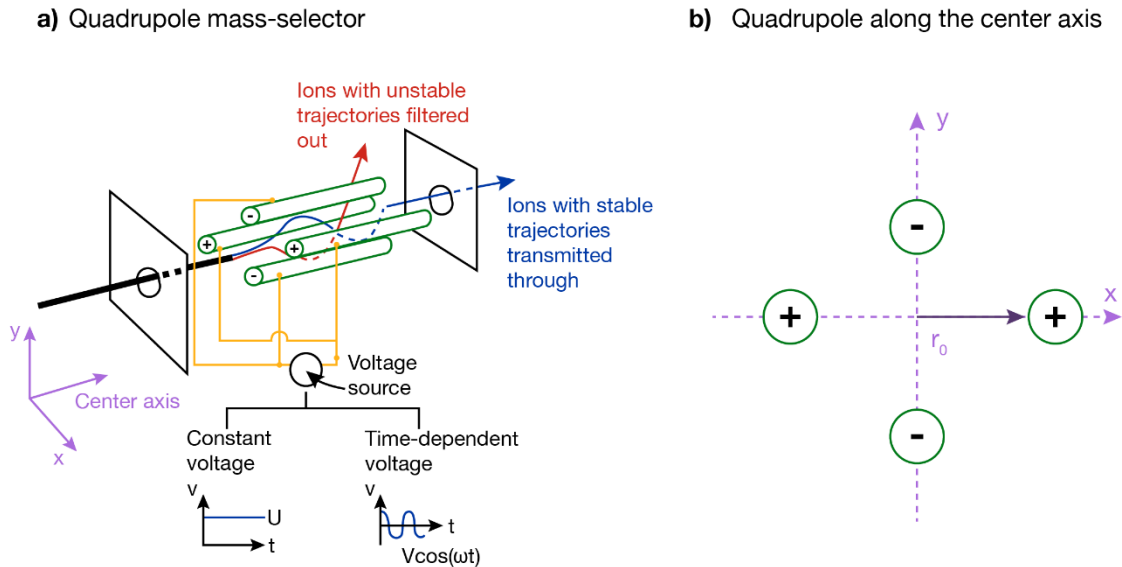
1146 A quadrupole mass selector typically refers to an arrangement of four collinear cylindrical metal
1147 rods (Figure 3.6). Each opposing pair of rods are connected electrically such that voltages can be
1148 established between each pair of opposing rods. We apply some constant voltage, U , in addition
1149 to a time-dependent voltage, $V \cos(\omega t)$ (ω is the frequency of the time-dependent voltage), to the
1150 rods in this arrangement. These voltages create an electric field in the space between the rods
1151 which can be approximated by the following equation:

$$\mathbf{E} = \frac{U + V \cos(\omega t)}{r_0^2} (-x\hat{\mathbf{x}} + y\hat{\mathbf{y}}) \quad (\text{Eq. 3.4})$$

1152 where r_0 is the (shortest) distance from the center axis of the quadrupole to the surface of the
1153 rods. Likewise, x and y are the distances from and perpendicular to this center axis, respectively.
1154 Note that the electric field along the center axis is zero. That is, there is only a non-zero electric
1155 field in the xy plane.

1156

1157



1158

1159 **Figure 3.6 | Schematic diagram of a quadrupole mass-selector.** (Left) This instrument consists of four
1160 long cylindrical rods arranged parallel to one another with each two opposing rods in electrical contact with
1161 one another. Depending on the constant and time-dependent voltages applied between the rods, particles
1162 can have either a stable trajectory through the quadrupole or an unstable trajectory and are filtered out.
1163 (Right) A view of the quadrupole along the center axis.

1164

1165 Substituting Eq. 3.4 into Eq. 3.3 will lead to differential equations known as Mathieu's differential
1166 equation:

$$\frac{d^2 u}{d\xi^2} + [a_u + 2q_u \cos(2\xi)]u = 0 \quad (\text{Eq. 3.5})$$

1167 Here, we have rewritten our original equation with $\xi = t/2$, $a_u = (4zU/\omega^2 r_0^2 m)$, $q_u =$
1168 $(2zV/\omega^2 r_0^2 m)$, and where u can represent either x or y .

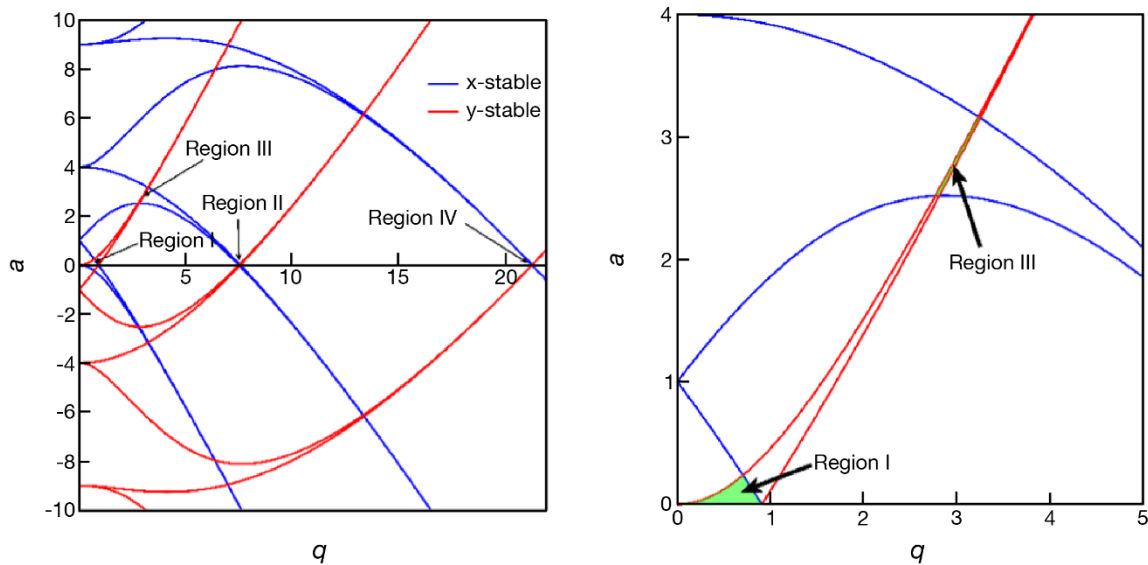
1169

1170 What does solving this equation give us?

1171

1172 Well, if we set $u = x$, the solution to this equation allows us to determine the values of $a_{u=x}$ and
 1173 $q_{u=x}$ where a particle has a stable motion along the x -axis. In this context, a stable motion just
 1174 means that the particle motion along the x -axis remains within the quadrupoles. But, for a particle
 1175 to be able to exit the quadrupole on the other side, we need it to have stable motion along both
 1176 the x -axis and the y -axis. So, we need to solve Eq. 3.5 for $u = y$ as well, giving us the values of
 1177 $a_{u=y}$ and $q_{u=y}$ where a particle has a stable motion along the y -axis. Plotting the region of values
 1178 for a and q for which the particle has a stable motion along the x -axis or the y -axis results in a
 1179 plot like that shown in Figure 3.7 (left). Where the regions overlap gives the values for a and q for
 1180 which the particle has a stable motion along *both* the x -axis *and* the y -axis (regions I, II, III and IV
 1181 in Figure 3.7). Outside these regions, the particle will end up leaving the quadrupole partway and
 1182 hit some wall somewhere (Figure 3.6). Now, if we know these values for a 's and q 's (such that
 1183 the particle has a stable motion) we can calculate what voltages, U and V , we need to apply to
 1184 the quadrupoles for a desired molecule with specific m/z value to go through our quadrupole (we
 1185 use $a = (4zU/\omega^2r_0^2m)$, $q = (2zV/\omega^2r_0^2m)$).

1186



1187

1188 **Figure 3.7 | $a - q$ stability diagram.** The plot shows the values of a and q for which the trajectory of an
1189 ion through a quadrupole is stable along the x -axis (x stable) and the y -axis (y stable). The regions where
1190 the x -stable and y -stable plots overlap give the stability regions where the ion trajectory is stable along both
1191 the x -axis and the y -axis simultaneously. These overlap regions, regions I, II, III, and IV, refer to the first,
1192 second, third, and fourth stability regions, respectively. Right: zoomed-in stability diagram near the origin.
1193

1194 **3.4.3. First stability region**

1195

1196 In practice, we often only focus on the first stability region (region I in Figure 3.7). Since both a
1197 and q are proportional to U and V , respectively, large voltages will need to be applied to the
1198 quadrupoles to operate within the other stability regions (regions II, III or IV). Of course, this
1199 depends on the frequency, ω , of the applied voltage. Typically, frequencies of 0.5 – 2 MHz are
1200 used. In this case, it is difficult to maintain large voltages (e.g., ~1kV) at such high frequencies
1201 due to hardware electronic limitations. Furthermore, large voltages should be avoided to avoid
1202 any electrical arcs forming between the quadrupoles in vacuum (Paschen's law).

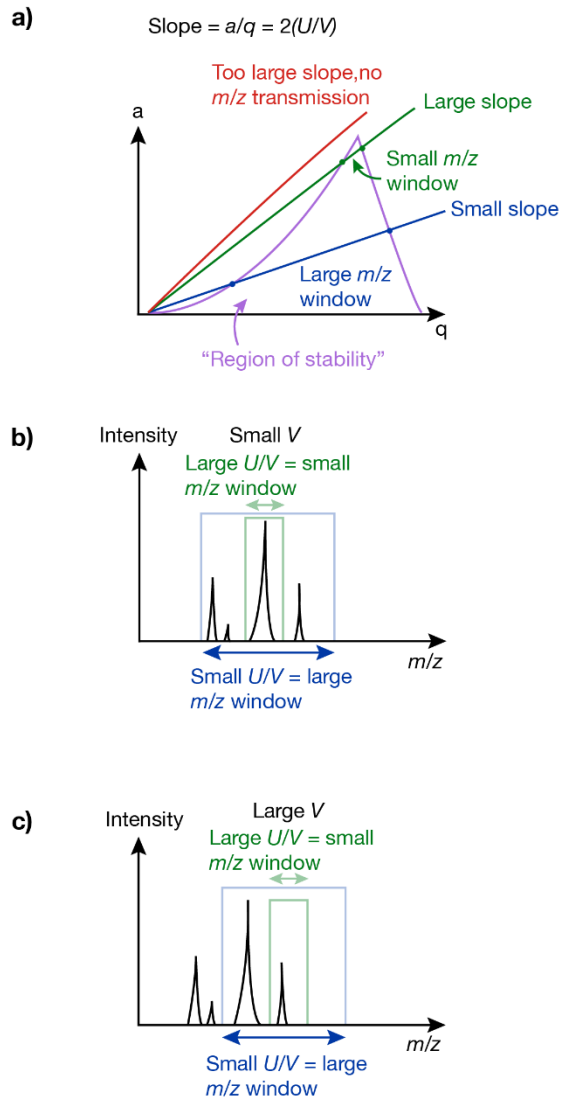
1203

1204 Keeping to the first stability region, we can control the range of m/z 's to let through the
1205 quadrupole. We do this by controlling the ratio of the voltages, U/V , that we apply to the
1206 quadrupoles. The U/V ratio defines a line that cuts through the first stability region (Figure 3.8),
1207 where the intersection points between the line and the region of stability defines the lowest and
1208 highest m/z the ions can have to be transmitted through the quadrupole.

1209

1210 A small U/V ratio means that we have a line with a less steep slope cutting the region of stability
1211 (Figure 3.8, blue line), since $a/q = 2(U/V)$. The intersection of the blue line with the region of
1212 stability gives the large range of m/z to be transmitted through. If we now set U and V such that
1213 U/V is large, the line cutting the region of stability has a steeper slope (Figure 3.8, green line).
1214 Here, the green line cuts a smaller portion of the region and therefore allows only molecules with

1215 a small range of m/z through the quadrupole. By making the ratio U/V higher, we can narrow the
 1216 window of m/z that molecules are allowed to have if they want to make it to the other side of the
 1217 quadrupole. However, setting U/V too high effectively forbids any molecule from exiting the
 1218 quadrupole (Figure 3.8, red line).
 1219



1220
 1221 **Figure 3.8 | Parameters that allow and prohibit ions to pass through a quadrupole.** (a) By adjusting
 1222 the ratio of applied voltages to the quadrupoles, U/V , we can control the range of m/z values for which
 1223 molecules can travel through the mass-selector. A higher U/V means a very narrow m/z window. While the

1224 ratio U/V changes the width of the m/z window, the value of the time-dependent voltage, V (keeping U/V),
1225 shifts the window to (b) lower m/z for smaller V and to (c) higher m/z for larger V .

1226

1227 Experimentally, we set a high U/V ratio such that the width of the m/z window that is allowed
1228 through is small (it can be as small as ± 1 atomic mass unit per charge) and then we adjust V
1229 (while keeping U/V constant) until our window is centered on the desired m/z that we want to
1230 transmit through the quadrupole. A lower V means a smaller m/z while a higher V means a larger
1231 m/z (Figure 3.8; bottom). The maximum applied V therefore defines the maximum m/z that we
1232 can measure for a fixed frequency, ω .

1233

1234 **3.4.4. Trade-offs**

1235

1236 In practice, the straightforward design and easy maintenance of the quadrupole device make it
1237 often the go-to when it comes to mass-selection. The small form factor (sizes typically on the
1238 order of centimeters) makes it convenient to use in a complex vacuum system. Though, some
1239 consideration should be made with regards to how compact the quadrupole should be. A small r_0
1240 will not allow sufficient space for ions to separate in space. Furthermore, the theoretical treatment
1241 of the quadrupole implicitly assumes that the quadrupoles are infinite in length where the charged
1242 particles are exposed to an infinite number of cycles of a time-varying voltage, $V \cos(\omega t)$. In
1243 reality, the finite length of the quadrupole can have a real impact on the resolution of the mass-
1244 selection: longer quadrupoles will improve the resolution of mass-selection, however,
1245 simultaneously, decrease the transmission of molecules through the quadrupole.

1246

1247 Further deviations from theory include the fact that the mass windows do not have a sharp m/z
1248 cutoff but rather a sloped cut-off. This means that a high-resolution operating mode of the
1249 quadrupole can inevitably lead to a decrease in ion transmission through the quadrupole and

1250 therefore lead to low ion current at deposition stage and hence prohibitively long deposition time.
1251 Beyond the design of the quadrupoles, the operation and m/z window of the quadrupoles relies
1252 not just on the values of the voltages applied but how stably these voltages can be maintained.
1253 Thus, while the design of the quadrupole is simple, the electronics required to maintain a highly
1254 stable voltage signal to the rods can become a limiting factor. The more stable the signal, the
1255 more expensive the electronic hardware required.

1256

1257 **3.5 Read these next**

1258

1259 **1. Detailed discussion on vacuum physics from theory to practice:** Modern Vacuum Physics.
1260 CRC Press (2004).

1261 **2. A textbook including principles and operations of mass analyzers:** Mass spectrometry: a
1262 textbook. Springer Science & Business Media (2006).

1263 **3. Detailed discussion into quadrupole-based mass separation:** Computer Simulation of the
1264 Mass Filter for a Finite Length Quadrupole. Commun. Mass Spectrom. 11, 184 (1997).

1265

1266 **Chapter 4. The soft landing**

1267

1268 **4.1. Introduction: Parachuting ions onto surfaces**

1269

1270 Alright, now that we have sent our molecules flying and have mass selected them, it is time to
1271 land them on surfaces! In other words, we need to catch a flying object on a surface.

1272

1273 How would you do this? How would you catch a fast flying object?

1274

1275 Well, clearly, we first need to know how *fast* we are talking about. Typical ions in an ESIBD
1276 instrument fly with a ~50 eV of kinetic energy.

1277

1278 This is *fast*.

1279

1280 For a 100-Da molecule (e.g., a small organic molecule), this is 9800 *meters per second*. For a 10-
1281 kDa molecule (e.g., a small protein), this is 980 *meters per second*. As a reference, an airplane
1282 that brings you around the world flies at a mere 230 *meters per second*. Ions are thereby flying at
1283 incredible speeds in an ESIBD instrument, and we need to find ways to bring them onto a surface
1284 – stationary and intact.

1285

1286 Now, as we want the ion to be *stationary* on surface at the end of the day, this means that we
1287 need to reduce the speed of the ions flying at these incredible speeds to zero. While this can
1288 certainly be achieved by simply putting a surface in the flight path of the ions, this will end up
1289 badly for the ions, as they will crash on the surface and break apart into fragments. Think about
1290 this: imagine what happens when your phone falls from the third-floor balcony onto the ground?

1291 Well, you will witness the breakup of your phone into pieces – and worry if it can be turned on
1292 again after you reassemble them.

1293

1294 So, how can we bring the ions onto a surface without destroying them?

1295

1296 Well, we need a strategy to lower the speed of incoming ions before they come in contact with
1297 the surface. By doing so, we will land them intact on surface – we will **soft land** them on surface.

1298

1299 The ESIBD technique relies on soft landing to deposit molecular ions intact on surface to ensure
1300 that the species adsorbed on surface is identical to the species mass-selected in the gas phase.

1301 However, soft landing is merely one regime out of the vast possibilities offered by the ESIBD
1302 technique as it allows ions to be deposited on surface with energies ranging from near zero to
1303 few hundred eVs (depending on the design of the deposition stage).

1304

1305 Hence, in the following sections, we present a model of ion deposition to flesh out all important
1306 parameters in bringing molecules from gas phase onto surfaces. This includes how to change the
1307 kinetic energies of ions approaching the surface, how to understand molecular excitations caused
1308 by molecules colliding with a surface, and how to decide what kinetic energies and surface
1309 conditions to use to achieve specific outcomes.

1310

1311 **4.2. How it works: Setting the touchdown speed and direction**

1312

1313 First, let us look at what is involved in a molecule-surface collision. When two objects collide, their
1314 collision outcome is dictated by the collision energy, collision angle, and impact parameter. The
1315 collision energy tells you how much kinetic energy is involved in the collision, the collision angle

1316 tells you the direction by which these two objects approach one another, and finally the impact
1317 parameter tells you the distance by how much the two objects miss one another.

1318

1319 Now, in the context of molecule-surface collision, the surface is considered to be at rest while the
1320 molecule approaches the surface from the gas phase. Hence, the collision energy refers to the
1321 kinetic energy of the molecule approaching the surface; the collision angle refers to the direction
1322 of how the molecule approaches the surface; and the impact parameter refers to the contact site
1323 of the molecule on surface, whether it lands directly above a surface atom or on the space
1324 between two surface atoms, and so on.

1325

1326 Today, collision energy and angle are two parameters we can control reliably in ESIBD
1327 experiments, while no strategy exists to control impact parameter of molecule-surface collisions.
1328 We thereby describe how to control the collision energy and angle in ion deposition experiments
1329 below.

1330

1331 **4.2.1. Collision energy**

1332

1333 Collision energy in a molecule-surface collision refers to the kinetic energy of the molecule
1334 approaching the surface i.e., the *translational* kinetic energy of the molecule. But, why should we
1335 care about it? Taking real world examples, you can already imagine what happens if you
1336 accidentally drop your phone on the floor from your sofa versus from your third-floor balcony.
1337 From the sofa, nothing happens. But from the balcony, your phone shatters into pieces. Control
1338 of collision energy is hence key to control the collision outcome.

1339

1340 The collision energy is most commonly varied in ion-surface collision by using electric field to
1341 accelerate or slow down the incident molecular ion.

1342

1343 Consider an example, if we want to slow down a positive ion with 50 eV kinetic energy, we should
1344 have the ion travel from a point with 0 V potential (point A) to another point with higher potential
1345 (say, +40 V – call it point B). In this case, the ion will decelerate due to the electric field caused
1346 by the 0 to +40 V potential difference (Figure 4.1). In effect, this converts the ion's kinetic energy
1347 (KE) into the electrostatic potential energy (PE) of the ion as much as:

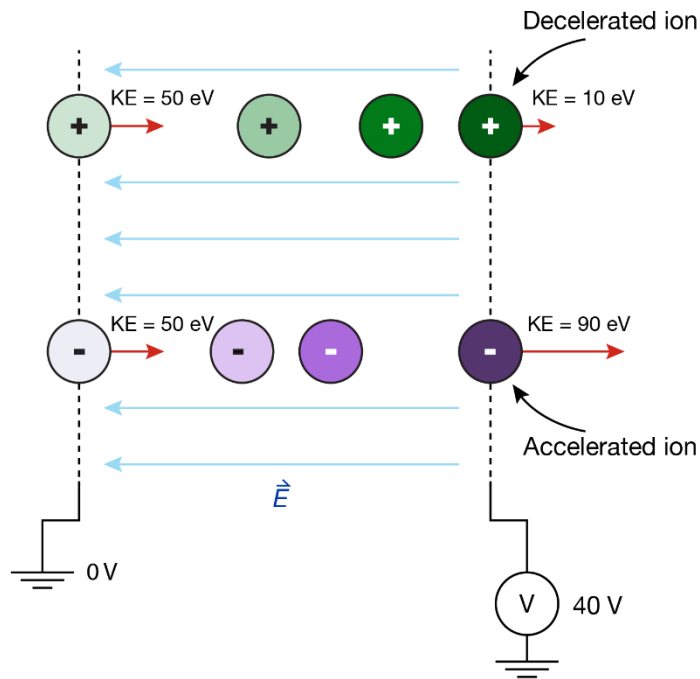
$$\Delta PE = z(V_{final} - V_{initial}) \quad (\text{Eq. 4.1})$$

1348 Arranging this equation to yield final ion kinetic energy gives the following expression:

$$KE_{final} = KE_{initial} - z(V_{final} - V_{initial}) \quad (\text{Eq. 4.2})$$

1349 Hence, for a positive ion with $z = +1 e$, going from point A ($V_{initial} = 0 \text{ V}$) to B ($V_{final} = +40 \text{ V}$) converts
1350 40 eV of the ion kinetic energy to its electrostatic potential energy, leaving the ion at point B still
1351 moving forward with 10 eV of kinetic energy (Figure 4.1, green ion). For an ion with $z = -1 e$, the
1352 opposite happens! The ion will be accelerated instead, such that at point B, the ion moves forward
1353 with 90 eV of kinetic energy (Figure 4.1, purple ion). Altogether these examples show how ion
1354 kinetic energy can be lowered or increased simply by changing the electric potential surrounding
1355 the ion. Details on how to implement this in an experiment are outlined in section 4.4.

1356



1357

1358 **Figure 4.1 | Acceleration and deceleration of ions by electric field.** Positive ions are decelerated when
 1359 brought to a region with a higher electric potential, while negative ions are accelerated when brought to a
 1360 region with a higher electric potential.

1361

1362 4.2.2. Collision angle

1363

1364 Collision angle in a molecule-surface collision can be defined by the approach angle of the ion
 1365 toward the surface relative to a reference, such as the surface plane. Now, again, why do we
 1366 need to care about collision angle? Going back to real world examples, do you recall what
 1367 happens when we throw a stone to a pond at a near-parallel angle versus at a perpendicular
 1368 angle? At a near-parallel angle, the stone will skip across the water, while at a perpendicular
 1369 angle, the stone will sink immediately. This case demonstrates the importance of controlling
 1370 collision angle to influence the collision outcome.

1371

1372 The simplest way to vary collision angle is by rotating the surface so that the ion beam impinges
1373 the surface at a desired angle.

1374

1375 **4.3. What happens to ions during and after landing?**

1376

1377 Now, let us consider what molecular motions and surface motions (i.e., dynamics) are initiated
1378 when a molecule collides with a surface.

1379

1380 At the fundamental level, collision is an event that distributes energy between collision partners.
1381 Hence in a molecule-surface collision, initial translational energy of a molecule approaching a
1382 surface is distributed into the kinetic energies of diverse molecular and surface dynamics. But,
1383 what dynamics are exactly excited from this?

1384

1385 Before we jump in, let us clarify what “molecular dynamics” and “surface dynamics” mean. Here,
1386 molecular dynamics refers to any internal motion in molecules, such as molecular rotation, bond
1387 vibration, bond bending, bond twisting, bond breaking, and so on. Surface dynamics refers to
1388 internal motion on surfaces, such as rippling (think of water ripples formed when a stone hits a
1389 pool of water), shearing, disintegration, and so on. Which molecular and surface dynamics are
1390 excited by a collision ultimately depends on the initial parameters of the molecule-surface
1391 collision, that is, collision energy, angle, impact parameters, and of course the identity of the
1392 incoming molecule. It is these collision-induced dynamics that dictate the outcome of any
1393 molecule-surface collision.

1394

1395 Now let us follow the journey of a molecular ion from gas phase onto a surface.

1396

1397 The first event that happens even before the molecule touches the surface is electron based. As
1398 a molecular ion approaches a surface within distances that allow electron tunneling (~1 nm or
1399 lower), a molecular ion may end up adsorbed on the surface as a charged molecule – or as a
1400 neutral molecule. Electron transfer can happen from the surface to the incoming molecular ion or
1401 vice versa depending on how the work function of the surface compares to the energy level of
1402 molecular orbitals. Here, work function refers to the energy required to remove an electron from
1403 a surface.

1404
1405 If the lowest unoccupied molecular orbitals (LUMOs) of the incoming ion are lower in energy than
1406 the occupied states of the surface, then one or more electrons could be transferred from the
1407 surface to the incoming ion, effectively increasing the number of electrons in the ion. Alternatively,
1408 if the highest occupied molecular orbitals (HOMOs) of the incoming ion are higher in energy than
1409 the unoccupied states of the surface, then one or more electrons could be transferred from the
1410 incoming ion to the surface, effectively decreasing the number of electrons in the ion. When both
1411 conditions are not satisfied, the ion retains the number of electrons it has in the gas phase when
1412 it adsorbs on the surface. We understand that through these molecule-to-surface or surface-to-
1413 molecule electron transfers, a molecular ion from the gas phase may end up as a neutral molecule
1414 on a surface.

1415
1416 Next, let us look at the ion dynamics as it touches the surface.

1417
1418 The dynamics could be largely categorized into impulsive and thermal dynamics. Impulsive
1419 dynamics (also known as non-equilibrium dynamics) refers to molecular motions where energy is
1420 largely present in a few specific types of molecular motions, while thermal dynamics (also known
1421 as equilibrium dynamics) is understood as motions where energy is distributed equally among all
1422 possible molecular motions. Following the first contact between an incoming molecule and a

1423 surface, the first few picosecond (10^{-12} s) of the dynamics is governed by impulsive dynamics,
1424 which eventually weakens and are replaced by thermal dynamics within a few nanoseconds (10^{-9}
1425 s). But, what exactly are these impulsive dynamics and thermal dynamics in the context of
1426 molecules and surfaces?

1427

1428 From the molecular viewpoint, the main impulsive dynamics are compression and shearing,
1429 whose proportions depend on the collision angle. When molecules collide perpendicular to the
1430 surface, they experience compressive forces. Alternatively, when molecules collide near parallel
1431 to the surface, they experience shear forces. Such molecular compression and shearing may
1432 break covalent bonds or non-covalent interactions (e.g., hydrogen bonds) to give mechanically
1433 induced chemical reactions or conformation changes, depending on the extents of compression
1434 and shearing. These extents depend on the energy of the molecule-surface collision. On top of
1435 inducing compression and shearing, higher collision energies could cause molecules to bounce
1436 back to the gas phase, while lower collision energies could help molecules to adsorb on surfaces.
1437 The exact values of these energies strongly depend on the surface reactivity, as we will detail in
1438 section 4.4.

1439

1440 Following the impulsive dynamics operative within first few picoseconds, thermal dynamics begin
1441 to dominate. Energy associated with molecular compression and shearing begins to spread to
1442 other motions, where, within few nanoseconds, this energy spreads almost uniformly among
1443 every atom in the system (molecule and surface). Following the complete redistribution of collision
1444 energy, the adsorbed molecules are fully governed by their dynamics on surface such as their
1445 diffusion on surface, their rotation on surface, and so on, detailed in section 4.4.

1446

1447 From the surface viewpoint, the collision creates pressure waves that travel away from the
1448 collision site, along the surface plane and also into the bulk of the surface. These waves are

1449 identical to ripples formed in a pool of water when you throw a stone into it. As collision energy
1450 increases, these shockwaves increase in amplitude, which at some point, is strong enough to
1451 break bonds between the surface atoms. Notably the extent of energy that can be adsorbed by
1452 the surface depends on the surface rigidity, detailed in section 4.4. As an analogy, a bouncy ball
1453 responds very differently when dropped on a pool of sand or on a ceramic floor.

1454

1455 **4.4. Soft landing in practice**

1456

1457 Now that we have a model of molecule-surface collision in our mind, it is time to dive into real
1458 practice. At this point, we should have a mass-selected ion beam aimed toward a surface. Three
1459 decisions need to be made before starting a deposition experiment: (i) the landing energy of ions,
1460 (ii) the deposition time, and (iii) the surface choice.

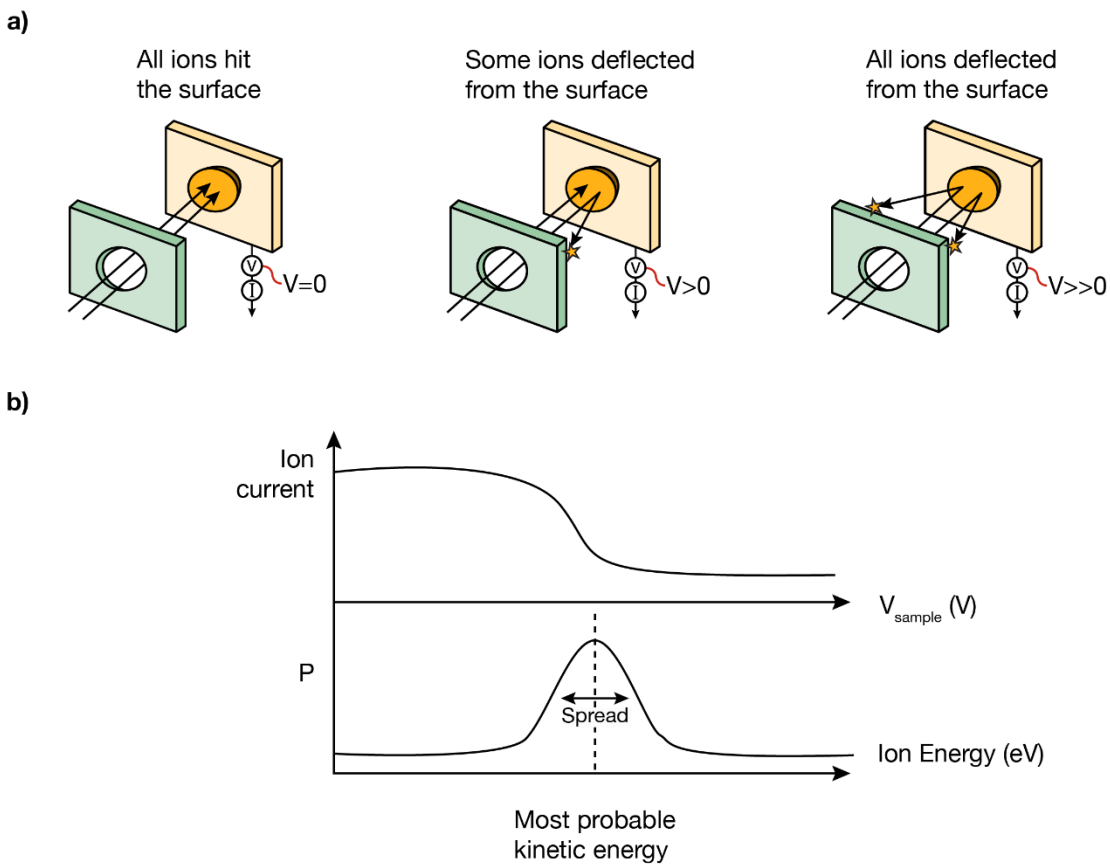
1461

1462 **4.4.1. The landing energy**

1463

1464 Setting the landing energy, that is the collision energy of the ions onto surface, involves two steps:
1465 (i) sweep the surface bias to measure the kinetic energy of ions, and (ii) set the appropriate
1466 surface bias so that the ions land on the surface with the desired energy. Step (i) is accomplished
1467 by measuring the ion current arriving from the ion beam aimed perpendicularly toward a surface
1468 while changing the voltages applied to that surface (called retarding voltages). By increasing the
1469 retarding voltages, we expect the ion current reaching the surface to decrease to zero at some
1470 large retarding voltage as now all ions are completely repelled by the surface (Figure 4.2a). This
1471 measurement of the ion current as a function of retarding voltage gives a sigmoidal curve (Figure
1472 4.2b). The first derivative of this curve yields the energy distribution of the ions in the ion beam
1473 (Figure 4.2b), allowing us to determine the most probable kinetic energy of the ions as well as its

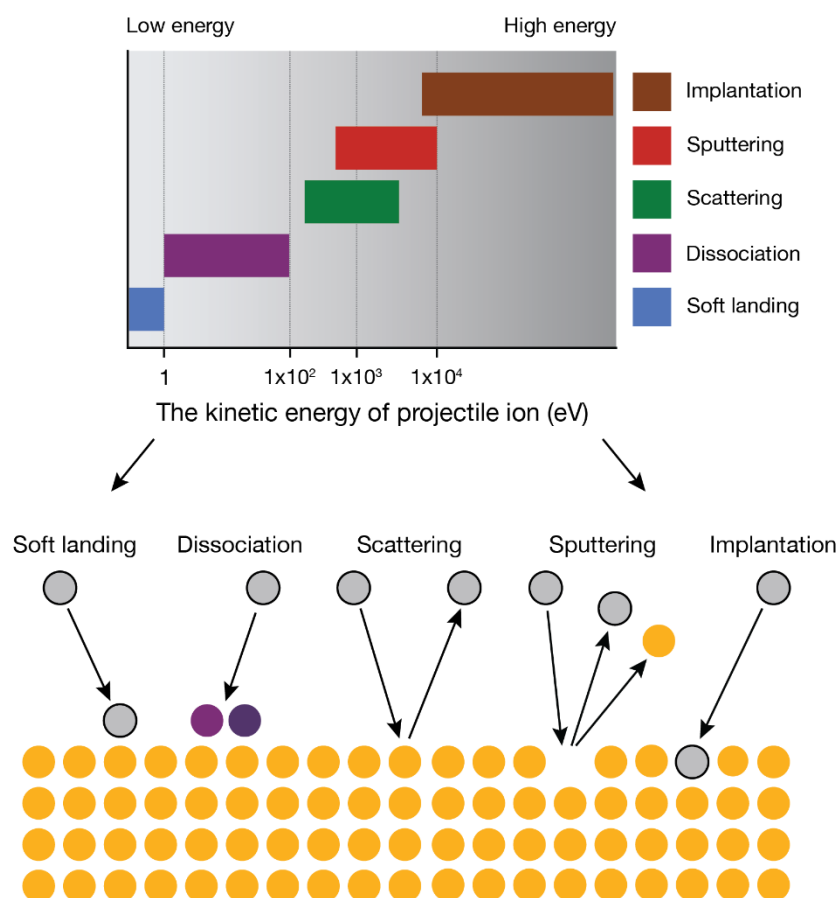
1474 spread. Next, on step (ii), the desired landing energy is set by applying an appropriate voltage to
 1475 the target surface. For example, if we have an $[M+2H]^{+2}$ ion flying at 100 eV kinetic energy and
 1476 we want to land this ion with 1 eV landing energy at the surface, then we need to set +49.5 V on
 1477 the surface, following equation 4.2.
 1478



1479
 1480 **Figure 4.2 | Instrument setup for ion deposition.** Panel (a) shows the effect of increasing retarding
 1481 voltage on the ion motion (here assumed to be positive ions). Panel (b) shows a typical sigmoidal curve of
 1482 current vs retarding voltage obtained from an energy measurement, and the first derivative of this sigmoidal
 1483 curve which yields the distribution of ion kinetic energy per ion charge.

1484
 1485 The landing energy is critical to the outcome of the molecule-surface collision event (Figure 4.3).
 1486 However, the choice of collision energy should consider the size of the molecular ion that you

1487 want to deposit. Given that kinetic energy is proportional to the molecular mass and, by that
 1488 extension, to the number of atoms, the choice of kinetic energy should be normalized to either
 1489 the molecular mass or the number of atoms. So far, for molecular ions landing on metal surfaces,
 1490 landing energies of ~ 4 meV/atom (or ~ 300 m/s) allow gas phase molecules to preserve their
 1491 structures upon landing on surface, ~ 40 meV/atom (or ~ 980 m/s) could cause molecules to
 1492 change their conformation upon molecular landing, and ~ 80 meV/atom (or ~ 1500 m/s) are
 1493 sufficient to induce chemical reaction upon molecular landing.
 1494



1495
 1496 **Figure 4.3 | Ion-surface collision effects.** The different ion-surface collision outcomes are illustrated
 1497 according to the level of kinetic energy. Credit: Adapted with permission of Annual Reviews, from Jacobs,
 1498 D.C.; Reactive Collisions of Hyperthermal Energy Molecular Ions with Solid Surfaces. *Annual Review of*

1499 *Physical Chemistry*. **2002**, 53, 379-407. DOI: 10.1146/annurev.physchem.53.100301.131622; permission
1500 conveyed through Copyright Clearance Center.

1501

1502 **4.4.2. The deposition time**

1503

1504 Once we know the landing energy, it is time to decide how much ions you want on a surface. Do
1505 you want to have a sub-monolayer, monolayer, or even multilayer coverage? These
1506 considerations will give you a target coverage denoted by the number of molecules per unit area,
1507 which can be used to calculate how much total ions you should deposit on surface.

1508

1509 Let us consider an example. Suppose that you want to have a sub-monolayer coverage of $[M+H]^+$
1510 molecules of around 1 molecule per $100 \times 100 \text{ nm}^2$. For a circular surface with a radius of 0.2
1511 mm, this corresponds to a total of 1.2×10^{11} molecules on the surface. With an ion current of 20
1512 pA arriving at the surface, this corresponds to a deposition time of 17 minutes (0.28 hour).

1513

1514 **4.4.3. The surface choice**

1515

1516 Finally, the choice of the surface comes into play. Four parameters are worth considering here:
1517 (i) surface conductivity; (ii) surface thickness, (iii) surface reactivity, and (iv) surface temperature.

1518

1519 First, the surface conductivity must be taken into account as we are landing ions on surfaces.
1520 Insulating surfaces may lead to charging issues. As more ions arrive on the surface, the electric
1521 potential starts to build up to the point that it may be enough to repel the incoming ions, preventing
1522 these additional ions from landing on the surface. Hence, the use of conductive surfaces (e.g.,
1523 metal surfaces) is important to ensure deposition of significant ions on the surface as well as to
1524 allow measurement of ion current from ions that arrive on the surface.

1525

1526 Second, surface thickness is critical to ensure compatibility with the goal of the deposition
1527 experiment. If you want to image the deposited molecules with SPM, *thick* metal surfaces are
1528 often used in UHV-based SPM while graphite (i.e., HOPG – highly ordered pyrolytic graphite)
1529 surfaces are common for ambient SPM. If you want to image the deposited molecules with
1530 electron microscopy, *thin* film substrates are used such as freestanding single layer graphene or
1531 amorphous carbon.

1532

1533 **Sidebar text box:** Scanning probe microscopy (SPM) versus electron microscopy (EM). SPM and EM have
1534 similarities and differences in their sample requirements due to their unique imaging mechanisms. In both
1535 SPM and EM, the sample should be made as rigid as possible to prevent any mechanical vibration that
1536 create artifacts in the imaging process. An SPM image is formed by moving a tip over a surface at a very
1537 small (<1 nanometer) tip-surface distance to measure a signal (e.g., electric current, force between tip and
1538 surface, etc.) at every X and Y coordinates on the surface. In the case of EM imaging, an image is formed
1539 by scattering a beam of electrons aimed toward a sample. Any vibration from loose parts of the sample
1540 (e.g., a loose screw on sample plate or a loosely held crystal on a sample plate) would create artifacts in
1541 both SPM and EM images. In SPM, vibrations would change the tip position and the tip-sample distance,
1542 while in EM, vibrations would change the area where the electron beam hits the sample. On top of these,
1543 common EM imaging mode (i.e., image generated by electrons that penetrate through a sample) requires
1544 the sample to be as thin as possible (ideally below 50 nanometers, and no more than 100 nanometers).
1545 For more details, we refer the reader to the literature (Bian, K., Gerber, C., Heinrich, A.J. *et al.* Scanning
1546 probe microscopy. *Nat Rev Methods Primers* 1, 36 (2021). <https://doi.org/10.1038/s43586-021-00033-2>;
1547 Ayache, J., Beaunier, L., Boumendil, J. et al. *Sample Preparation Handbook for Transmission Electron*
1548 *Microscopy*. Springer, New York, NY (2010). <https://doi.org/10.1007/978-1-4419-5975-1>).

1549

1550 The thickness of the surface also determines its mechanical rigidity, influencing the outcome of
1551 the deposition. To imagine this, think of what happens when you land on a trampoline (thin, flexible
1552 surface) versus when you land on a ceramic floor (thick, rigid surface). For example, gas phase
1553 structures of proteins are preserved by landing them on flexible, single atom thick graphene; while
1554 some structural changes occur when folded proteins are landed on rigid crystal surfaces of metals

1555 or insulators. Notably, hard surfaces could also be coated with soft matter (such as polymers or
1556 self-assembled monolayers) to cushion molecules landing on these surfaces.

1557

1558 Second, surface reactivity is important in dictating what happens to the deposited molecules after
1559 they arrive on the surface. Molecules adsorbed on a surface could undergo non-reactive events,

1560 such as diffusion or conformation change, as well as reactive events, such as dissociation or
1561 reaction with other adsorbed molecules to give new molecular species on surface (Figure 4.4).

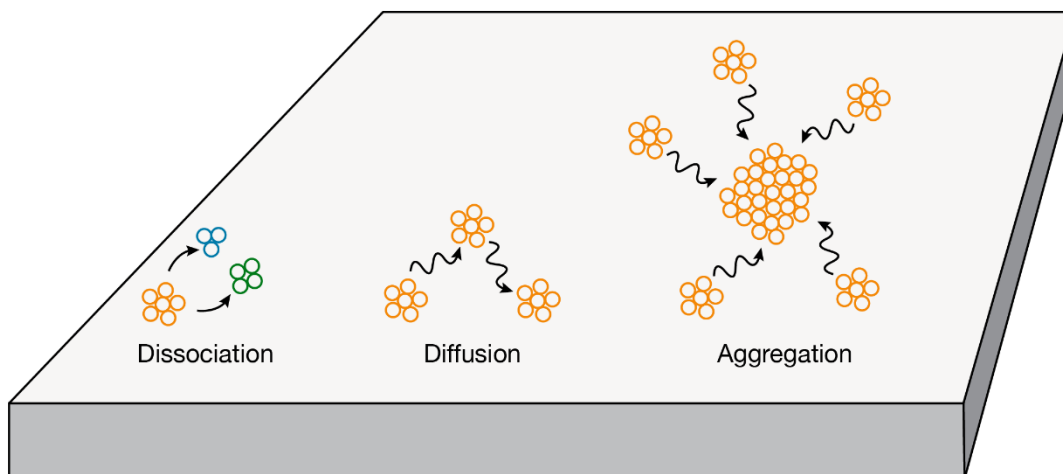
1562 Consider highly reactive silicon surfaces, e.g., Si(100) or Si(111), against inert metal surfaces,
1563 e.g., Au(111). In contrast to Au surfaces, silicon surfaces are extremely reactive due to presence

1564 of dangling bonds, causing the surface to form covalent bond with any atoms or molecules
1565 adsorbed on it, effectively anchoring them on the surface. As a *heuristic*, here we sort common

1566 surfaces in surface science experiments from the most reactive to the least reactive: Si, Ir, Pd,
1567 Cu, Ag, Au, NaCl, graphene, graphite. For noble metal surfaces, (110) facet tends to be the most

1568 reactive while (111) facet tends to be the least reactive, with (100) facet lies somewhere in
1569 between.

1570



1571

1572 **Figure 4.4 | What do molecules do on surfaces?** Molecules on a surface could diffuse or aggregate into
1573 molecular islands. These adsorbed molecules could also dissociate or react with other molecules on the
1574 surface to give new molecular species.

1575

1576 The choice of surface ultimately depends on the goal of the experiment. For single molecule
1577 analysis by SPM, an ideal surface should be sufficiently reactive to limit molecular mobility on
1578 surface by increasing its diffusion barrier (otherwise, molecules will diffuse and form 2D molecular
1579 islands on surface), but also sufficiently inert so that the deposited molecules do not chemically
1580 react further into something else. Our experience finds that Cu(100), Cu(111), and Ag(110) hits
1581 the balance required for such experiments. For material synthesis, an ideal surface should be
1582 inert to encourage high mobility of deposited molecules so that they form large islands of
1583 assembled molecules. Common surfaces used here are inert surfaces, such as graphite,
1584 graphene, Au(111) surfaces, or surfaces decorated with self-assembled monolayers.

1585

1586 Finally, surface temperature is an important parameter that dictates whether adsorbed molecules
1587 have sufficient energy to overcome the barrier for various molecular processes on surface (Figure
1588 4.4). For single molecule analysis, deposition of ions on cold surfaces is often desired to
1589 deactivate any molecular diffusion on surface. Given that activation barriers for molecular diffusion
1590 are often smaller than that for chemical reactions, deposition on cold surfaces also ensures that
1591 molecules do not further react chemically after being adsorbed on the surface, thus ensuring that
1592 the identity of molecules on surface remains the same as that in the gas phase. For material
1593 synthesis on surfaces, elevated temperature may be desired to encourage molecules to diffuse
1594 and react with one another on surfaces, and also to give enough energy for molecules on surface
1595 to arrive at their most thermodynamically stable states.

1596

1597 Overall, the combination of surface thickness, surface reactivity, and surface temperature provide
1598 a wealth of parameters to achieve your experiment goals.

1599 **4.5 [Insert Insider: How do you use soft landing of mass-selected ions in your lab?]**

1600

1601 **4.6. The future of the field**

1602

1603 This primer has described the role of ESIBD in empowering the field of single molecule
1604 microscopy and surface science. The soft landing technology has also found remarkable success
1605 in advancing material sciences (see the Insider Q&A video in section 4.5). Also, very recently,
1606 ESIBD has found success in interfacing with the field of cryo-electron microscopy, allowing the
1607 three-dimensional gas phase structures of proteins to be imaged in real space. We anticipate that
1608 ESIBD could find ripe areas of exploration when coupled with recent ion manipulation techniques
1609 in tandem mass spectrometry.

1610

1611 Building on top of section 1.4, we hereby speculate several additional directions where
1612 explorations remain scarce. (i) Soft landing on insulators. This could be realized by performing
1613 the ion landing in non-vacuum environment (e.g., in 1 mbar of Ar), allowing ions on surface to be
1614 “solvated” with noble gases to form a “Coulomb crystal” like assembly on surfaces – or
1615 alternatively, concurrent deposition of positive and negative ions could be envisioned. (ii) Optical
1616 control of ion state prior to soft landing. Quantum state of molecular ions could be manipulated
1617 via laser pulses prior to their soft landing, thereby attaining quantum state-dependent soft landing.
1618 (iii) Soft landing on liquids. This could lead to nanostructures at gas-liquid interfaces, which could
1619 allow unique properties of gas-liquid interface to be realized (e.g., nanostructures formed by soft
1620 landed ions at the gas-liquid interface could be used to control evaporation rates of different
1621 dissolved gases in liquids). These speculative directions paint an exciting future that awaits the
1622 soft landing technology.

1623

1624 **4.7 [Insert INSIDER - What is the future of this field?]**

1625

1626 **4.8. Read these next**

1627

1628 **1. Detailed discussion on ion-surface collision dynamics: (a)** Reactive collisions of
1629 hyperthermal energy molecular ions with solid surfaces. *Annu. Rev. Phys. Chem.* 53, 379 (2002).

1630 **(b)** Fast Molecular Compression by a Hyperthermal Collision Gives Bond-Selective
1631 Mechanochemistry. *Phys. Rev. Lett.* 126, 056001 (2021). **(c)** Exploring the Molecular
1632 Conformation Space by Soft Molecule–Surface Collision. *J. Am. Chem. Soc.* 142, 21420 (2020).

1633 **(d)** Landing Proteins on Graphene Trampoline Preserves Their Gas-Phase Folding on the
1634 Surface. *ACS Cent. Sci.* 9, 151 (2023).

1635 **2. Fundamentals of surface chemistry:** Introduction to Surface Chemistry and Catalysis. ISBN:
1636 978-0-470-50823-7 (2010).

1637 **3. Other areas of ion soft landing:** Soft-Landing of Peptides onto Self-Assembled Monolayer
1638 Surfaces. *J. Phys. Chem. A.* 4, 1678–1687 (2006).

1639 **4. Proof of principle of ESIBD+cryoEM:** Cryo-EM of soft-landed β -galactosidase: Gas-phase
1640 and native structures are remarkably similar. *Sci. Adv.* 10, ead14628 (2024).

1641 **5. Ion manipulation techniques in gas phase:** The Omnitrap Platform: A Versatile Segmented
1642 Linear Ion Trap for Multidimensional Multiple-Stage Tandem Mass Spectrometry. *J. Am. Soc.*
1643 *Mass Spectrom.* 33, 1990 (2022).